Reply to referee comment #01

We appreciate the kind words on our manuscript and thank the reviewer for the constructive comments and proposed suggestions. These helped to substantially improve the manuscript. Please note that we changed figures 1, 2, 7, 8, 10, 12 based on comments of the reviewers. We also added an appendix in which we briefly describe the idealized model setup in more detail.
We will answer to all comments of reviewer #01 below point by point. Referee comments are given in bold, answers in standard, and changes to the manuscript in italic font.

The paper is very well written, the analysis is thorough and convincing. It's one of those manuscripts that seem to anticipate the reader's questions and answer them. And I really like the photo in Fig. 2! I think that the study is suitable for publication in ACP almost as is. I only have very few, mainly technical comments.

Minor comments:

P2. L14-17. I'm confused about the terminology here. In my reading of, e.g. Birner and Bönish 2011 and Abalos et al. 2017 the distinction between the shallow and deep branches of the Brewer-Dobson circulation is not identical with a separation between mean advection in mixing. Rather, the shallow branch transport is comprised of both two-way eddy mixing and slower advection by the residual circulation, the two largely balancing each other. The definitions of the two branches have more to do with transit times, stratospheric entry regions, etc. Am I wrong on this? It may be true that it is eddy mixing that connects the tropics with the high latitudes (as in Krause et al.) but in the region considered in the present manuscript, with latitudes south of 60N it seems the mean advection also plays a role. All this is tangential to the subject of this study and all I mean is that the terminology used here doesn't seem consistent with the literature. Also, I think that Birner and Bönish 2011 could be cited here.

Thanks for pointing this out. Of course, the shallow branch consists not only of two-way eddy mixing but also advection by the residual circulation.
We changed the text here as follows also taking into account the comments of reviewer #2:

"The stratospheric circulation contributes with two distinct branches distinguished based on the transit time between the major entry point of air into the stratosphere, i.e., the tropical tropopause, and the extratropics. The so called deep branch, i.e., associated with long transit times affects the ExTL through the descent of old stratospheric ozone rich air into the UTLS. In contrast, the shallow branch with significantly shorter transit times introduces relatively young air from the tropical and subtropical UTLS into the extratropical UTLS (Birner and Bönisch, 2011). A recent study based on airborne measurements showed the effect of these two transport pathways on the changing abundance of carbon monoxide (CO) over the course of the Arctic winter in the ExTL (Krause et al., 2018)."

P6 L13. The description of the COSMO model could use just a little more detail. It's a regional model, right? Where do the boundary conditions come from? Also, define the acronym (I believe, Consortium for Small-scale

Modeling)

We initially kept this description brief, because it is a repetition of Kunkel et al. (2014, 2016) and we wanted only to provide the most necessary details to follow the discussion later in the manuscript. However, since both reviewers ask for more details, we extended the description of the COSMO model setup in the revised version and added more details to the new Appendix A.

P16 L15. I think it should be stated explicitly what this classical meaning is. This comes up again below in Section 3.3.

At this point the classical meaning of TST is exactly what the reviewer suggests in the next comment, i.e., an air parcel irreversibly crossing the tropopause from the troposphere into the stratosphere (as indicated by changing PV). However, although we think that our measurements show that air parcels from the troposphere must have entered the stratosphere, the trajectories are not that clear. In our trajectory analysis we do not find a coherent ensemble of trajectories entering the stratosphere just once and then staying there. We rather find trajectories coming from the troposphere, thus carrying a tropospheric chemical signature, which cross the tropopause multiple times. Note, that Wernli and Bourqui (2002, their Figure 1) introduced a residence time criterion which accounts for such multiple changes. The question remains whether this back and forth is something that happens as such in nature or whether this is potentially indicative for a gradual transition between the troposphere and stratosphere. Another option is of course that this behavior is rather an artifact due to the inability of the model to represent this situation entirely correct. For further clarification we rephrase this paragraph as follows:

“Thus, for further discussion we rather omit the terminology of TST and STT trajectories in a sense of coherent ensembles of trajectories which cross the tropopause only once from the troposphere (stratosphere) to the stratosphere (troposphere) (Wernli and Davies, 1997; Stohl et al., 2003). We rather think of trajectories which show the potential of mixing around the tropopause by encountering low Richardson numbers and having PV values changing between tropospheric and stratospheric values, nevertheless leading to a subsequent exchange across the tropopause.“

P19. L14-17. Again, I’m confused about the “classical” STE and how it’s opposed to what we have here. Isn’t “an air parcel crossing the dynamic tropopause” the one and only meaning of TST? Does this sentence simply mean to say that we can’t tell, based on the trajectory analysis, whether a STE event has occurred or not but the analysis provides evidence that it has? Maybe it’s just a matter of defining things more clearly. Also, I would say “classical sense” instead of “classical meaning”; just a preference.

Here and according to the comments above we change parts of the paragraph to:

“However, based on the trajectory analysis it is difficult to estimate whether STE and in particular TST occurs in a way that air parcels cross the dynamic tropopause

only once from the troposphere into the stratosphere and stay there afterwards. We also performed longer trajectory calculations which, however, also provide no further evidence of TST trajectories which then stay in the stratosphere. We rather find trajectories which, based on PV, alternate back and forth between troposphere and stratosphere and which encounter low Richardson numbers along their paths. One potential reason why no TST trajectories are found which stay in the stratosphere is that the model fails to correctly resolve the process. "

Technical corrections

P4 L11. The acronym 'TIL' is introduced here but later "tropopause inversion layer" it is almost always spelled out throughout the paper. It should just be "TIL" from now on.

We changed tropopause inversion layer to TIL on the following pages.

P3 L17. "All processes which lead to cross tropopause transport of air parcels have one common impact on this air parcel," There's something grammatically wrong with this sentence

We changed this sentence to:

"An air parcel crossing the tropopause has to be affected by processes which can modify its potential vorticity (Hoskins et al., 1985). Only then the air parcel can enter from a region with generally low PV, i.e., the troposphere, into a region of high PV, i.e., the stratosphere or vice versa."

P4 L14 initial → initially

Changed as suggested.

P6 L4. forecast →forecasts

Changed as suggest.

P7 L13, "in this study we use the 2 pvu isosurface as dynamic tropopause" this was already stated in the first paragraph of section 2.3. I suggest deleting this sentence.

We deleted this sentence.

P9 L5. "(Figures 1c,d)" Should it be 1c,e?

Correct. However, since we modified Figure 1, this part refers now to Figures 1b,c.

P10 L14-L16 This sentence a little awkward. It talks about crossing the tropopause above the tropopause, which doesn't make sense to me!

We changed this sentence to:

“At FL 380 HALO was initially flying in the lowermost stratosphere, then gradually approaching and finally crossing the dynamic tropopause which was slightly tilted according to the ECMWF analysis (Figure 3a).“

Fig 3a caption. Richardson number contour is not mentioned in the caption.

We added the description to the caption.

P10 L33. “defincies” → deficiencies(?)

Correct. We changed it accordingly.

P12 L5. “seek for” → seek (or search for)

Correct. We changed it accordingly.

Figure 4 Caption. I think the symbols Q M and Q should be swapped. Also, lrt1 (first lapse rate tropopause) is not described in the caption or discussed in the text.

Thanks for pointing this out. We corrected the symbols and we included the description of lrt1 to the figure caption. In the text it is now also referred to the lrt1. We also note that we kept the lrt1 because in this figure it nicely shows how close the lrt1 and dynamic tropopause are in this case.

P20 L9. 240.000. I think you want a comma there: 240,000

True. Changed it accordingly.

P20 L13. Propability → probability.

Correct. We changed it accordingly.

P23 L 10 passoing → passing
Correct. We changed it accordingly.

References:
Wernli, H. and Bourqui, M.: A Lagrangian “1-year climatology” of (deep) cross-tropopause exchange in the extratropical Northern Hemisphere, J. Geophys. Res., 107(D2), 4021, doi:10.1029/2001JD000812, 2002.

Reply to referee comment #02

We appreciate the careful reading of our manuscript by the reviewer and thank the reviewer for the constructive comments and proposed suggestions. These helped to substantially improve the manuscript. Please note that we changed figures 1, 2, 7, 8, 10, 12 based on comments of the reviewers. We also added an appendix in which we briefly describe the idealized model setup in more detail.
We will answer to all comments of reviewer #01 below point by point. Referee comments are given in bold, answers in standard, and changes to the manuscript in italic font.

Major concerns

1. **Dynamic vs. thermal tropopause: Both definitions of the tropopause are used in the study, whereby I think that the authors are more inclined to the dynamic tropopause – which is OK. Still, I wonder why both definitions are needed for this study because the two definitions agree in a climatological sense, but locally the two tropopause heights can differ substantially. This, for instance, is the case where tropopause folds occur. I would therefore appreciate if the role of the two tropopause definitions is more clearly discussed.**

   Thanks for pointing out this issue. Generally, as the reviewer noticed, in terms of STE we are more inclined to the dynamic tropopause, most specifically because its definition based on potential vorticity and the associated conservation law which to first order is often fulfilled close to the tropopause. On the other the hand, the static stability is a thermodynamic quantity related to the temperature of the atmosphere. More specifically, the enhanced values of static stability are associated with the temperature inversion which is commonly found above the lapse rate tropopause. One goal of WISE was to study whether STE occurs in the vicinity of enhanced static stability. From our point of view it is then necessary to have an eye on both the lapse rate and potential vorticity based tropopause in our discussion. However, to avoid further confusion and since the focus of the study is on mixing and potential STE we will generally refer to the dynamic tropopause in the manuscript and only use the lapse rate tropopause when necessary. This will then also be highlighted explicitly in the text.
   To clarify things more, we will add a sentence in the manuscript at the end of Section 2.4:

   "Finally, note that in this study discussion around static stability are usually associated with the lapse rate tropopause, while discussion about STE are linked to the dynamic tropopause. Thus, both definitions will be considered in the analysis, however, if only the term tropopause is used, then we refer to the dynamic tropopause with a value of 2 pvu throughout the manuscript."

   More specifically,

   P2,L32: Here it is written that 'these results are independent of the definition of the tropopause'. What exactly is meant by 'these results'?

   These results referred to the spatial and temporal occurrence of STE. We changed the text accordingly:

“Also in a climatological sense the occurrence of STE in the extratropics is independent of the definition of the tropopause as shown by Boothe and Homeyer (2017) who used four different modern reanalysis data sets to analyze STE as well as lapse-rate and dynamic tropopause definitions.”

Figure 1 and corresponding text: In this figure, the local thermal tropopause is shown; but the dynamic tropopause is missing? Why? Actually, in the text (P7,L32) the measurement are discussed with respect to the height relative to the tropopause, without explicitly mentioning which definition of the tropopause is used (the thermal one; see figure 1) and ‘misleading’ the reader that the dynamic tropopause is used by mentioning the ‘stratospheric PV’ values (P7,L28), i.e. the key aspect of the dynamic tropopause.

The initial intention of Figure 01 was to give an overview of the synoptic situation. For this we decided to show PV and N^2 along with several quantities which from our point of view were relevant for our study. We also wanted to connect our story to the point where Kunkel et al. (2016) stopped their analysis with respect to the exchange. For this we started our discussion around STE (wrt to the dynamic tropopause) and enhanced stability (wrt to the lapse rate tropopause) to link these two features. However, since this apparently led to some confusion and to a too strong focus on the static stability, we decided to rearrange Figure 01. Now we mainly show the distribution of PV and start the discussion about static stability later in the text. Figure 03 also shows the most important features of static stability that were evident in the original Figures 01d,e. Static stability is only included as one of several contour lines in the revised Figure 01. Please note that the new Figure 1 has a slightly different color-scale for PV which has one value for negative PV values which occur for instance at the top of the WCB. Also tropospheric values (on the Northern Hemisphere and based on our dynamic tropopause definition) are now represented by one value/one color, so that the dynamic tropopause is more easily detectable than before. The color-scale then increases by 0.5 pvu from 2 pvu to 10.5 pvu to illustrate the high PV variability in the lowermost stratosphere. We hope that this and the general clarification on the term tropopause as described above reduces the confusion about tropopause definitions.

Figure 01: Revised Figure 01, now focusing on potential vorticity to show the synoptic situation

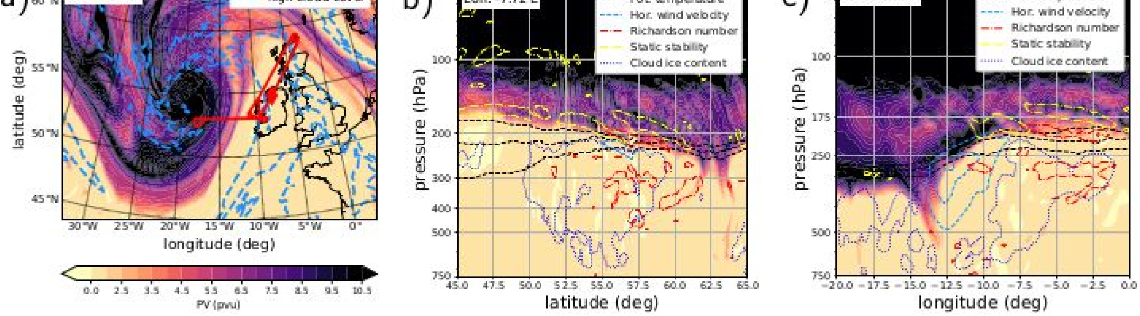

Figure 4 contains, in contrast, the dynamic and the thermal tropopause. Why?

Figure 4 shows time series of measured and modeled quantities, however, only along the flight path without any real two-dimensional information. The intention was to include both, lapse rate and dynamic tropopause, to show that in this case these two hardly differ. Since the TIL is directly linked to the lapse rate tropopause, the lrt1 can be further used as an indicator for the TIL location, while the dynamic tropopause gives a rough idea how deep HALO was flying in the stratosphere.

P21,L6-7: "We also find a spatial coincidence in the horizontal plane between the enhancement of N2 above the thermal tropopause and TST across the dynamic tropopause by analyzing passive tracers in our idealized simulations (Figure 10)." Here, both definitions of the tropopause are referred to. This is somewhat 'confusing' to me.

However, from our point of view it is necessary to show both, since STE is related to the dynamic and static stability rather to the lapse rate tropopause. As noted by the reviewer, thermal and dynamic tropopause can coincide but do not necessarily have to. This is for instance the case in the region of the trough. Following Figure 10 we included a cross section in Figure 11. There it is shown that the two tropopause definitions coincide in altitude at the location of the exchange. This further indicates that the diagnosed exchange does not strongly depend on the tropopause definition in the current study.

2. **Streamlining the introduction: The introduction basically ‘offers’ everything that is needed for the study. But at some places I felt that a clear storyline was missing. Let me show this with some very specific examples:**

P2,L18 an L26: At both places it is written where STE occurs predominantly, i.e. it looks a little repetitive and the reader must read twice in which sense the two paragraphs differ.

We revised some of the paragraphs focusing on STE in the introduction. In particular, we shortened paragraph 2 and include the most relevant information in the fourth paragraph.

P3,L3-15: This paragraph discusses the crucial role of Rossby waves for STE, which I fully agree with. What I am missing is the link to the previous paragraph! As a reader I had the impression that this paragraph opens up a new story (Rossby waves), and does not ‘naturally’ evolve from the previous paragraph. Of course, this always reflects some personal view, but I think the introduction would benefit a lot if the story more clearly from one paragraph to the next.

The intention was that the paragraph starting on P2, L24 briefly discusses climatological features of STE, while the following paragraph lists the STE relevant processes in the extratropics. We start this paragraph now also with the following sentence:

“Within the storm tracks Rossby waves are crucial for STE.”

Hence, many processes (radiation, folds, clouds, convection, gravity waves) are introduced in the introduction, but they remain somewhat 'unrelated' to the main topic (ridges in baroclinic waves). To be sure, I think it is fine to mention all these different aspects, but the processes should be streamlined (or directed) towards the topic of the paper.

We agree that the introduction is comprehensive, in particular with the goal to cover all processes related to baroclinic waves which potentially lead to STE. We also wanted to make sure that although STE in the extratropics has been addressed quite comprehensively in the literature, we found a process which has not been discussed as it is done in the current study..

3. **Role of the enhanced stability above the tropopause: The storyline of the study is built around the enhanced stability near the extratropical tropopause and that STE is encountered in this region. While reading the text, I had the impression that a special role is attributed to this enhanced stability for STE. But there are several other processes at work: gravity waves (as discussed several times), turbulent regions due to lowered Richardson numbers.**
   In short, I wonder whether the whole story could also be interpreted in a different way, i.e. we encounter STE not because of the enhanced stability but despite of it. Then, the argument could be as follows: (i) a gravity wave evolves near or at the tropopause; (ii) because of this gravity wave vertical wind shears are increased and therefore the Richardson number becomes small; (iii) this reduction in the Richardson number due to the wind shear dominates any impact of the enhanced vertical stability and therefore leads to turbulent mixing and hence STE.
   I don’t know whether this is a valid interpretation of the current case, but it would see the enhanced vertical stability in a completely different light. I think the authors should discuss these alternative interpretations, or at least make clearer why the enhanced stability is so important for the mixing.

   Our intention was indeed to show that mixing occurs despite the enhanced static stability and not because of it. The line of argumentation outlined by the reviewer is fully valid and also follows the line of argumentation in the paper:
   i) a gravity wave is evident above the tropopause (Fig.3)
   ii) increased vertical wind shear and related reduction in Richardson number (Fig. 4)
   iii) the increased wind shear outweighs even the enhanced static stability found in the lower stratosphere in the regions of mixing (Fig 3, 4)
   Figure 5 shows observed indications of mixing. Figure 6 shows that small scale dynamic features seem to dominate the flow (i.e., the presence of the small scale waves) while Figure 7 and 8 extent the analysis and shed light onto the synoptic situation and a bit on the ability of the ECMWF model and kinematic trajectory models running on this data to capture this process.
   Section 4 was then designed to i) further analyze and generalize the findings presented in Section 3 and ii) extend the analysis of Kunkel et al. (2016).
   As stated above in the revised manuscript we changed Figure 01 to reduce the initial focus on static stability.

Another point is the question that is placed in the 7th paragraph of the introduction (P4, L12). We change this question as follows:

“Does STE occur and does it affect the formation of the ExTL in the ridge of baroclinic waves where the static stability is usually strong in the extratropical lowermost stratosphere?”

4. **Power spectral densities (Figure 6 and corresponding text): The power spectrum is discussed in Figure 6 to show that isotropic turbulence (k=-5/3) prevails for flight leg (FL380), but that geostrophic turbulence (k=-3) prevails at later flight legs. The discussion should be clearer and in particular, I would like the following aspects to be addressed:**

   Why is it possible to identify structures down to 100 m with a sampling frequency of 2-3 Hz? Is this simply given by the aircraft's speed and the sampling period?

   The 100 m rather correspond to the 10 Hz data provided by the BAHAMAS instrument of HALO, i.e. for temperature and wind. Along with an average ground speed of about 210 ms^{-1}, this would allow us to identify structures down to 100 m, taken into account that several independent measurement points are required to identify a structure. Of course, the trace gas measurements with about 3 Hz would not allow to identify such small structures.
   We changed the sentence on P15 L6-7 to make this clearer:

   “On board HALO the frequency of measurements is about 10 Hz for the state parameters such as temperature and wind, while it is about 2-3 Hz for CO and N_2O. Along with an average ground speed of about 210 ms^{-1} and with the 10 Hz measurements of the state parameters this potentially allows us to identify atmospheric structures down to about 100 m.”

   Is there a reference that a slope of k=-3 is typical for gravity waves, as stated in the text (P15,L14-15)? I am certainly not an expert on power spectra, but I would have expected geostrophic turbulence to be typical at larger scales?

   This last sentence is thought as a summary of this paragraph, summarizing the findings of the paragraph. As outlined in the text (P15, L10) a slope of k=-5/3 is thought to be characteristic for isotropic turbulence and k=-3 for geostrophic turbulence (P15, L13).
   We rephrased the last sentence to make it clearer that this sentence is thought as a summary of the power spectral density discussion:

   “Summarizing, close to the tropopause the slope of k=-5/3 suggests that meso-scale processes, e.g., related to gravity waves, might be substantial to explain the dynamics in the tropopause region.”

   The slope k=-3 (red line) seems to apply for a range between 0.01 and 0.2 Hz,whereas for smaller and larger frequencies it clearly deviates from this behavior (in figure 6b). How has this to be interpreted?

The slope of k=-3 is evident to about 1 Hz, if it is taken into account that there is a sort of offset at around 0.2 Hz. Afterwards the spectral density flats out, which could be sign of simply missing meso-scale features while other larger scale features become more relevant again which are, however, not fully resolved by our measurements.

Basically, I think it is nice to have the power spectra in the manuscript, but I would appreciate a more detailed discussion.

We appreciate the interest in the power spectral density. Our intention was to show that turbulent motions occurred in the vicinity of the tropopause which have their sources in processes on the meso scale. In contrast, these processes seem to have no relevance farther away from the tropopause. The power spectral densities in Figure 6 nicely show this behaviour for the two considered legs (FL380 and FL420). Of course, the power spectral densities allow for a much deeper analysis, which is however, beyond the scope of the current manuscript but is the focus on current ongoing analyses which will then cover the power spectral densities in more detail.

5. **Idealized simulations: In section 4, the authors refer to an idealized baroclinic life cycle simulation in Kunkel et al. (2016), more specifically to the experiment BRTC LC1. Of course, I understand that not all details of this previous simulation can be given. However, I would appreciate as a reader if could read (and understand!) the current paper without having read Kunkel et al. (2016) -- simply because I could not remember. Hence, I think that the authors should include as much details from Kunkel et al. (2016) in the current study that it becomes understandable without the previous study, i.e. it becomes more or less self contained.**
   As a specific example, In P20,L17 it is stated that STE starts to occur slightly after the time of the first enhancement of N^2. But where exactly is this N^2 value determined? I might have missed it in the current text, or it might indeed have to be got from Kunkel et al. (2016).

   We understand that the discussion of the idealized life cycles is probably too short in the current manuscript since this issue has been addressed by both reviewers. We thus decided to give a more comprehensive description of the model setup in an appendix. We also added some more information on how the N^2_{max} is traced during the barolinic life cycle experiment to the caption of Figure 9.

Minor comments:

P2,L5: “certain trace species” -> You might want to specify already at this place what trace species are meant.

We change this to:

“...distributions of trace species such as CO, O_3, H_2O, or N_2O with either distinct tropospheric or stratospheric….”

P2,L6-78: Would it make sense to give, in addition to the height range above and below the dynamical tropopause, also in hPa or m?

Hoor et al. (2004) does not give a height range in hPa or m, from Hegglin et al. (2009) the top of the ExTL was estimated to be about 2 km above the dynamical tropopause based on CO-O_3 correlations. However, there is no fixed relation between geometric altitude and potential temperature, this depends rather on the time and space varying vertical gradient of potential temperature. This in turn is highly dependent on the synoptic situation. Thus, any numbers in geometric space are relatively vague and are associated with larger uncertainty (see Hoor et al. (2004) and Hegglin et al. (2009)). Because of this we rather keep the initial formulation, only giving the range for potential temperature.

P2,L13: "in the deep branch into the UTLS" -> It is not immediately clear by the term 'deep branch', in particular if a reader is not very familiar with STE. It might be helpful to introduce in 1-2 sentences the stratospheric circulation with the distinct branches.

Following the suggestions of both reviewers we changed this paragraph accordingly:

"*The stratospheric circulation contributes with two distinct branches distinguished based on the transit time between the major entry point of air into the stratosphere, i.e., the tropical tropopause, and the extratropics. The so called deep branch, i.e., associated with long transit times affects the ExTL through the descent of old stratospheric ozone rich air into the UTLS. In contrast, the shallow branch with significantly shorter transit times introduces relatively young air from the tropical and subtropical UTLS into the extratropical UTLS (Birner and Bönisch, 2011). A recent study based on airborne measurements showed the effect of these two transport pathways on the changing abundance of carbon monoxide (CO) over the course of the Arctic winter in the ExTL (Krause et al., 2018).*"

P2,L16: "two competing transport pathways" -> Why are the two pathways competing? In which sense are they competing?

See last comment, we removed the competing.

P3,L19-20: "Lamarque and Hess (1994) separated between diabatic, i.e., potential temperature changing, and diffusive, i.e., related to friction, processes and showed that diabatic processes play a more vital role for STE than diffusive processes." -> Are there newer studies showing that diabatic processes than diffusive ones? I wonder whether this applies to STT and TST, and I am really not convinced that turbulent mixing is less important (in particular for STT)?

We fully agree that turbulence might have been underestimated in older studies. A potential explanation is that processes leading to turbulence in the UTLS have been poorly treated in models in these studies. An example is that Gray (2006) found similar results as Lamarque and Hess (1994) with cloud and radiative diabatic effects dominating over turbulent processes with respect to STE. In contrast, a recent study by Spreitzer et al. (2019) who by applying a Lagrangian technique could show that turbulence plays a major role in changing PV around the tropopause in the ridge of an extratropical cyclone and that cloud related diabatic processes are more relevant at lower tropopause altitudes. We extent the discussion here as follows:

“Lamarque and Hess (1994) separated between diabatic, i.e., potential temperature changing, and diffusive, i.e., related to friction, processes and showed that diabatic processes play a more vital role for STE than diffusive processes. Analyzing cross tropopause transport in the UKMO model Gray (2006) found similar results with cloud and radiative processes being more important for STE than processes related to turbulence. In contrast, a recent study by Spreitzer et al. (2019) shows that turbulent processes are mainly responsible for changing the PV around the tropopause in a ridge of an extratropical baroclinic wave. They used high resolution ECMWF forecast data and conclude that the turbulence is evident around the jet stream. This turbulence is mainly related to the vertical shear of the jetstream but can also be caused by gravity waves (Zhang et al. 2015a).”

P3,L24: "Clouds and related diabatic heating" -> What are the diabatic heating processes related to clouds? Does it refer in particular to condensational heating (phase changes of water and ice)? Or is radiative cooling at cloud top also relevant?

With “clouds and related diabatic heating” we refer to all diabatic processes related to clouds, that those triggered by phase transitions (condensation, evaporation, etc) but also radiative processes related to clouds, e.g., radiative cooling on top of clouds.

P3,L26-27: "... can reach the upper troposphere and modify the PV, consequently allowing for exchange between tropospheric and stratospheric air..." -> Note, however, that WCB air masses do not necessarily enter the stratosphere; the diabatic heating during the ascent is associated with mid-tropospheric PV changes, and the WCB is also able to modify the upper-level PV, but further diabatic and/or diffusive processes are needed that the air masses cross the tropopause.

We are aware that the ascent of WCB air masses does not necessarily end in the stratosphere. This is a rather uncommon process and additional processes are required to allow for STE (Madonna et al., 2014). As our study shows and as has been hypothesized in a previous study (Kunkel et al., 2016), there is a potential of air masses undergoing STE above the WCB outflow due to turbulent processes. In the current study the turbulence has been observed on top of the WCB outflow (Figure 2a) and the ECMWF model also predicts ice clouds up to the tropopause as it is the case in our idealized experiments. In Kunkel et al. (2016) it has been shown that the turbulent kinetic energy is enhanced on top of the ice clouds. Other numerical studies showed that clouds can substantially alter the PV structure at the tropopause, consequently allowing for STE (e.g., Gray, 2006, Lamarque and Hess, 1994, Spreitzer et al., 2019).

P4.L31+33: "took place" & "are to examine"; the tense is switching from past to present; please make this consistent (not only at this place).

Thanks for the hint, we checked the manuscript for further inconsistencies.

P5,L33-34: "had the goal to study the abundance of trace species in the extratropical tropopause region in relation to the occurrence of enhanced values of static stability in the lower stratosphere and to potential STE." -> Please rephrase in a clearer way; as a suggestion: ".. in the extratropical tropopause region and how they are influenced by the enhanced static stability ... and potential STE. Such conditions were found by Kunkel et al. (2016) to occur in the ridges of extratropical baroclinic waves. Therefore,…"

We changed this sentences to:

"The goal of research flight RF 07 on 28.09.2017 was to study the abundance of trace species in the extratropical tropopause region. In particular, in accordance to the major goals of the WISE mission, the focus of this flight was on whether the trace species show specific signs of recent STE in regions of enhanced values of static stability in the lower stratosphere. Furthermore, the design of this flight was chosen such that the predictions of the idealized simulations of Kunkel et al. (2016) could be supported by observations."

P6,L9: Why is a slightly degraded horizontal grid (0.125 deg) for the trajectory calculation compared to the other analysis (0.07 deg)?

The use of a slightly degraded grid was related to technical issues with the memory allocation why we had to choose a slightly lower resolution for the trajectory calculations. We note here that the differences between these two horizontal resolutions are almost negligible for our purposes.

P7,L7: The horizontal resolution of the COSMO output is 0.4 deg; in contrast, it is 0.125 deg for ECMWF, i.e. it is higher for ECMWF than for COSMO. Is this correct? How do the vertical spacing of ECMWF and COSMO compare in the UTLS?

This is correct, ECMWF has a finer horizontal grid spacing, but COSMO the finer vertical grid spacing with 110 m in the UTLS (P7, L7) compared to the ECMWF model with about 300 m in the UTLS (P6, L10).

Section: 3.1: Would it be possible to have one figure (or figure panel) where all flight legs are labeled? While reading this section it was difficult to immediately know where the flight legs are. For instance, it would help to locate the flight legs of figure 3 more easily.

Figure 2: Revised Figure 2a, now highlighting FL380 and FL420.

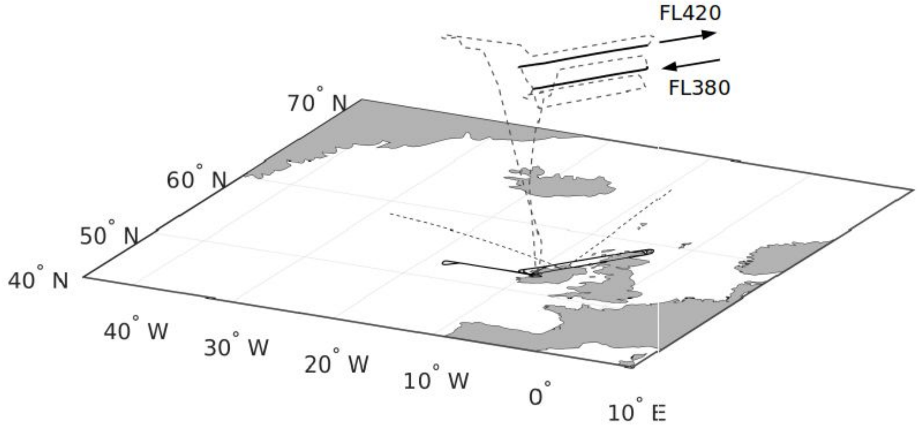

We revised Figure 2a and mark the two flight legs which most important for our study as shown above. The arrows point in the direction of the flight on the respective legs.

P10,L23-: Here, a model deficiency is discussed, namely the too high values of the Richardson number near some regions around the tropopause. This discussion of a model deficiency somewhat interrupts the main storyline, and hence I wonder whether it should better be discussed in section 2.2 where ECMWF data are introduced? Furthermore, the term 'in some regions' is rather unspecific, and immediately lets the reader ask where these regions are.

Since the discussion of the Ri-discrepancy is very specific and related to the details of Fig. 3, we decided to leave this at the position in the text. Otherwise a reader would have to go backward and forward in the manuscript, when discussing this later.
Please note that we change *“some regions”* to *“regions around the tropopause where the vertical shear of the horizontal wind is large”*.

P10,L34-35: "Thus, the model forecast underestimates the strength of the inversion, most potentially due to defincies in representing the gravity wave in this region." -> First, note the spelling error! Then, how sure are you that this is indeed a gravity wave? Then, the underestimation of the strength of the inversion is attributed to the effect of the gravity waves, i.e. because they are not well enough captured by the model. How do you know that this underestimation is not because of a limited vertical (and horizontal) resolution of the model?

Thanks for pointing out the spelling error. A limited grid spacing indeed would result in an underestimate of the inversion strengths and we suspect that this is mainly related to the vertical grid spacing. However, the occurrence of gravity waves under these meteorological conditions is shown in e.g. Kunkel et al. (2014, 2016) and confirmed by the GLORIA observations (Fig. 3b).
The gravity wave is not well captured in the ECMWF model due to the limited vertical and horizontal resolution of the model.
We change the text accordingly:

“Thus, the model forecast underestimates the strength of the inversion, potentially related to deficiencies in representing the gravity wave in this region due the still relatively coarse grid spacing in the UTLS.”

P13,L2-3: "In general, at the tropopause the CO−N2O correlation starts with larger CO and larger N2O mixing ratios at potential temperatures typical for the extratropical tropopause" > 'larger' refers to a comparison; but to what is it compared? Of course, I see the point, but I think it is not perfectly clear. Furthermore, I wonder whether it is correct to say that a correlation starts at a larger N2O and CO values. It sounds a little strange to me!

We change this sentence to:

"In general, at the tropopause the CO-N_2O correlation shows almost tropospheric mixing ratios of CO (~90 ppb_v) and N2O (~331 ppb_v) at potential temperature levels typical for the extratropical tropopause in the current case (~335 K)."

P16,L12: What does "at some time" mean? Or, stated otherwise: How long are the backward trajectories? Possibly, I simply missed this piece of information, and if not: Please add it!

The backward trajectories start at 01 UTC on 28.09.2019 and end at 11 UTC on 29.09.2019. With "some time" we refer to this time interval. We also note that there were wrong start and end dates provided in the text (P16, L14) which have been corrected accordingly and now agree with the times given in the caption of Figure 7. We rephrase this sentence on P16, L12 to:

"For this we filter all trajectories to find those trajectories which cross the dynamic tropopause and which encounter Richardson numbers smaller than 1 at any point in time during the period of the trajectory calculation."

P16,L23.24: " Starting from this region the trajectories strongly decelerate in a region of alternating horizontal divergence. During this time the trajectories cross back and forth over the dynamic tropopause." -> How do you see in figure 7 that the trajectories are decelerating? How do you interpret the alternating horizontal divergence? Is the divergence pattern due to the gravity wave?

The deceleration is not shown directly, but can be indirectly inferred from Fig 7c where the time around 15 UTC is shown. Trajectories have been calculated between 01 UTC on 28.09.2019 and 11 UTC on 29.09.2019 covering a time range of 34 hours. Figure 7c shows the time relative to 15 UTC on 28.09.2019 which is 14 hours after trajectory start but 20 h before the trajectory end time (thinking in physical time direction). However, the distance covered in the 14 hours before 15 UTC is much larger than the distance covered in the 20 hours after 15 UTC, thus the trajectories must have decelerated. The divergence is most probably related to the gravity wave.

P16,L26-27: " The motion back and forth across the chosen PV value for the dynamic tropopause becomes also evident from the PV along the trajectories (Figure 8a)." -> I am not sure whether I see this crossing back and forth over the dynamic tropopause in figure 8. What I see is that both sides (PV smaller and larger than 2 PVU) are 'covered' by the trajectories, but no further details.

We admit that the crossing of individual trajectories is not evident in Figure 8a. However, there is also no coherent ensemble of trajectories which crosses the tropopause only once and then stays in the stratosphere. Analyzing the PV values along the trajectories also provided the information that many trajectories cross the dynamic tropopause several times but not as a coherent ensemble oscillating around the dynamic tropopause..

We change the sentence accordingly:

“The analysis of the PV along the potential TST trajectories shows that these trajectories rather oscillate around the dynamic tropopause than cross the tropopause as coherent ensemble once and then reside in the lower stratosphere. This is somewhat evident in Figure 8a where only those trajectories are shown which at the physical start time of the trajectories have PV values smaller and at the last physical time step PV values larger than the respective dynamic tropopause PV value (here 2 pvu).”

Figure 7: In the text it is written that a transition (although not a smooth one) can be seen in the PV (panel b). This is difficult to see in my print out. It might also be helpful to have the relevant flight legs added to the figure; otherwise, it is a little 'difficult' to relate the trajectories to the measurements.

We altered the color scale of Figure 7b to improve the visualization of this behavior. Regarding the flight legs, the caption states of Figure 7 states: “Trajectories crossing the 2 pvu isosurface and encountering a dynamic instability which cross the flight track between 14:36 –14:48 UTC.” Thus, these are the trajectories which cross the flight track at FL380 between the respective time. We will add the information of the flight leg to the caption and hope that along with the new Figure 2a this helps to bring together all necessary information.

Figure 8: Why does the scale go up to 10 PVU in panel a)? In the same line, would it be possibly to adjust the scale in panel d)? Here, Ellrod and Knapp's TI index is shown as an additional turbulence indicator? Earlier in the text, only Richardson number was considered? I think it would be nice to be consistent throughout the manuscript, i.e. either to discuss only one or both indices. Finally, would it make sense to zoom in into a shorter time period around 15 UTC? For example, from -8 h to + 8 h.

We change the scale to go up only to 5 PVU in panel a) and to cover only the range of 330 K to 340 K in panel d).
We tend to keep the TI since the TI increases due to both horizontal deformation and/or vertical shear of the horizontal wind. If the TI is large this means that either one of these or both processes must be at work. If the TI is large and Ri is low, we can conclude that the vertical shear is large and causing the turbulence. Thus, this is another confirmation of our hypothesis that the mixing processes is caused by the strong shear of the wind.
In the revised manuscript we shorten the time period shown in Figure 8 and make it symmetric around 15 UTC. We now show the 14 hours prior and after 15 UTC to still demonstrate that the time around 15 UTC is rather unique.

P19,L3: Where does the number 69048 come from? Is this the starting frequency of the trajectories times the duration of the time period?

This is the number of trajectories started during the time period between 14:20 – 14:36 UTC.

P19,L14-23: Here, it is discussed whether the STE (and in particular TST) follows the classical meaning of TST. What is 'the classical meaning of TST'?

The term is unclear! Actually, I wonder whether this whole discussion about 'classical' or 'not classical' is necessary? If the authors would like to keep it, a more detailed discussion about the exact meaning of this term has to be included, and it has to be made more clear why it is relevant for the study.

We hope that we could clarify this issue also brought up by reviewer #01 and refer here to the answer given to reviewer #01. We changed the text here accordingly:

"However, based on the trajectory analysis it is difficult to estimate whether STE and in particular TST occurs in a way that air parcels cross the dynamic tropopause only once from the troposphere into the stratosphere and stay there afterwards. We also performed longer trajectory calculations which, however, also provide no further evidence of TST trajectories which then stay in the stratosphere. We rather find trajectories which, based on PV, alternate back and forth between troposphere and stratosphere and which encounter low Richardson numbers along their paths. One potential reason why no TST trajectories are found which stay in the stratosphere is that the model fails to correctly resolve the process. "

Figure 9 and the corresponding text: This figure shows the maximum static stability in the idealized baroclinic life cycle experiment BRTC LC1. I have several questions with respect to this figure: (i) How robust is the maximum static stability? (ii) Are only STT and TST trajectories in the ridges of a baroclinic wave included? I guess that this is not the case, but if so: It distracts the reader from the main story, which is about STE at exactly these locations.

Referring to (i): Several studies used the maximum static stability to identify the TIL (e.g., Erler and Wirth, 2011; Gettelman and Wang, 2015; Kaluza et al., 2019). Following Erler and Wirth, 2011 as well as Kunkel et al., 2014, 2016 we use the maximum static stability to trace the appearance of the TIL in the baroclinic life cycles which start from a state with no enhanced static stability but with a stratospheric background value of around 4.0×10^{-4} s^{-2}. To avoid to introduce spuriously high values we trace the maximum of the static stability which has been averaged over the first kilometer above the first local lapse rate tropopause. For this and based on previous analysis we think that N^2_{max} is a relatively robust measure of the evolution of the enhanced static stability in the life cycle experiments.
Referring to (ii): In this figure we show all TST and STT trajectories which makes from our point of view an even stronger point by not filtering by region. This filtering is done in the consequent figures. The point here is to show that there is a temporal coincidence between the N^2 enhancement, initiated by the updraft in the troposphere, i.e., the WCB, and the slightly delayed STE which is in line with the point made before that processes at the top of the WCB outflow can lead to STE. In the following figures we show that there is also a spatial coincidence first in the horizontal (Figure 10) and also in the vertical (Figure 11) between TST and N^2 enhancement in the ridge of the baroclinic wave.

P21,L3-4: "Thus, there is almost a temporal coincidence between the start of the enhancement of static stability and the first occurrence of STE." -> The statement is fine, but it repeats essentially the first sentence of the paragraph. Hence, it is somewhat repetitive!

We remove this sentence in the revised manuscript.

Figure 10: Where are these structures relative to the ridge and trough of the baroclinic wave?

In a revised Figure 10 (panels a and b) we include isolines of potential temperature for 315K and 325 K on the level of the dynamic tropopause to visualize the ridge and trough.

P22,L4-5: "In contrast to TST and although a temporal coincidence is also evident for N2 enhancement and occurrence of STT, no spatial co-occurrence is evident for STT in regions of enhanced N2 (Figures 10c,d)" -> Rephrase in a clearer way? How do you infer that STT does not co-occur with enhanced N^2? Is this statement based only on the blue area in figure 10? Wouldn't we need a stratospheric tracer to make such a statement?

We also have a stratospheric tracer but do not show this tracer in the manuscript. For completeness, we show the respective figures here. Please note that the first STT is diagnosed a few hours later than the first TST (see Figure 9). At 60 h after model start, there is also no stratospheric tracer evident at the first tropospheric level below the dynamical tropopause:

Figure 3: Stratospheric tracer on the first tropospheric model level below the dynamic tropopause. Black contour lines show values of static stability of $N^2 = 5.5 \times 10^{-4}\ s^{-2}$.

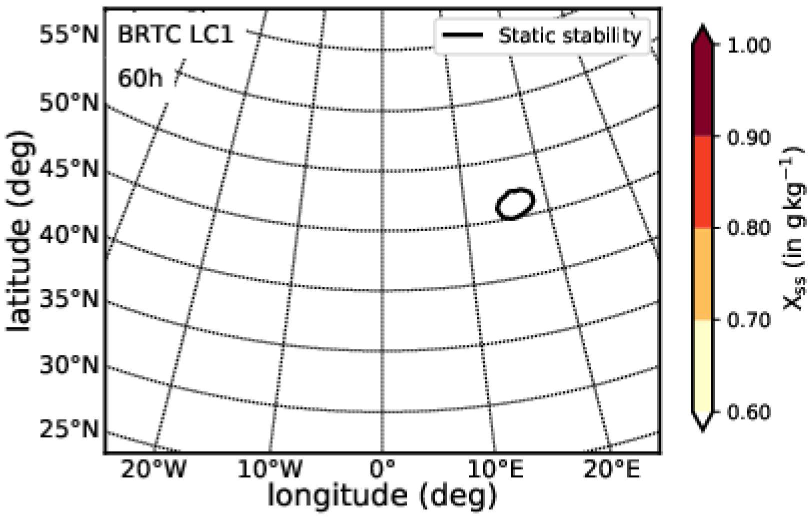

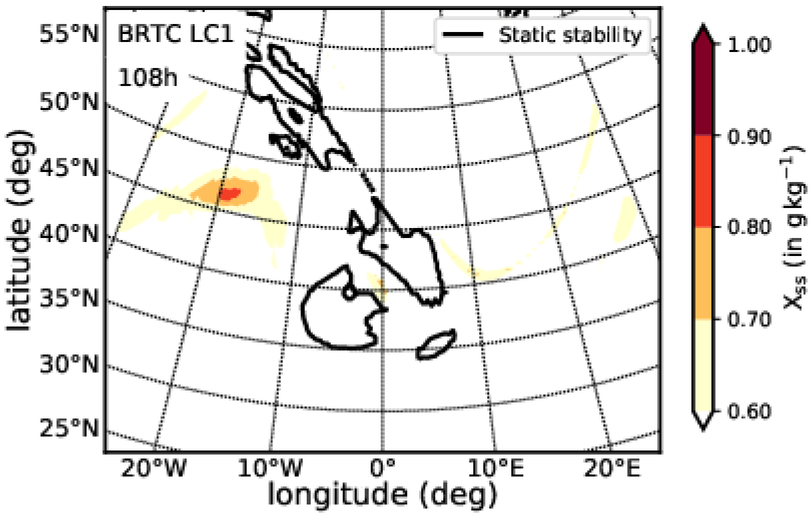

As well as there is a spatial overlap between the red areas of F10c,d with the tropospheric tracer, there is a spatial overlap between the blue areas and the stratospheric tracer.
We rephrase the respective sentence to:

"In contrast to TST and although a temporal coincidence is also evident for N^2 enhancement and occurrence of STT, no spatial co-occurrence is evident for STT in regions of enhanced N^2 (Figures 10c,d and also based on the analysis of the stratospheric tracer which is not shown explicitly here)."

P22,L8: "just above a region of ice cloud occurrence" -> What is the relevance of these ice clouds?

From Kunkel et al. (2016) it is known that these ice clouds increase the static stability in the lower stratosphere through radiative cooling. More so, these ice clouds show the location of the WCB and most importantly that the WCB reached up to the tropopause. Since in our observational case the clouds also reach up to the tropopause, this gives us more confidence that the idealized experiment strongly resembles the observations.
Regarding the process, on top of the ice clouds usually a radiative cooling is evident which can further enhance the static stability in the lower stratosphere. Also on top of the ice clouds there could be enhanced turbulence due to buoyant heat fluxes caused by strong gradients in total water. This is also addressed in Figures 14b,c.

P22,L9: "wave pattern related to a propagating inertia gravity wave" -> The gravity wave seems to be rather important for the mixing across the tropopause? It is not completely clear to me where this gravity wave originates from? Further, it is written that the wave propagates? But in which direction? It seems to me, based on the vertical cross sections, that the wave does not really propagate in the vertical direction. Instead, could it be that the gravity wave actually propagates along the troposphere-stratosphere interface, i.e. along the tropopause? A more refined analysis would be very helpful, given that the wave patterns is mentioned at several places in the manuscript.

The gravity wave is probably emitted from the upper tropospheric jet-front system, just as described for instance by Plougonven and Snyder (2007) or Wei and Zhang (2014). Such gravity waves, so called inertia gravity waves, tend to propagate more in the horizontal direction than mountain waves which mainly propagate vertically. From theoretical and idealized model studies it is known that these waves propagate in close vicinity to the tropopause where they can break or at least dissipate (e.g., Bühler and McIntyre, 2005; Plougonven and Snyder, 2005; Plougonven and Zhang, 2014).
However, from our observations we can not infer much about the wave, since we crossed it only once but do not know exactly how we crossed it in a geometric sense. And although the ECMWF model shows signs of the gravity wave, for instance in the divergence of the horizontal wind, we know from our analysis that the model does not capture this structure correctly as we see from the potential temperature along the flight track (Figure 4).

P26,L8-9: "A common feature of the two sets of trajectories is that in both cases the potential temperature values hardly change in the six hours; thus, the TST occurs quasi-isentropically." -> How do you see this in the figure? Or is this statement based on a quantitative analysis of the trajectories? I think a more detailed discussion of the quasi-isentropic transport is necessary, in particular because this is one of the key words in the article's title.

A detailed analysis (not shown) of the trajectories in Figure 8d shows that potential temperature of these trajectories changes about 1 K around the time of the TST but is otherwise almost constant. Also the trajectories in our idealized experiments hardly change their potential temperature, although slightly more than those shown in Figure 8. From Figure 12 this is evident by the almost constant color code along the individual dots of the individual trajectories. Further analysis showed that the potential temperature along these trajectories changes between 1.0-2.5 K over the course of the six hours.

References:
Bühler, O. and McIntyre, M. E.: Wave capture and wave–vortex duality, J. Fluid Mech., 534, 67–95, 2005.

Erler, A. R. and Wirth, V.: The Static Stability of the Tropopause Region in Adiabatic Baroclinic Life Cycle Experiments, J. Atmos. Sci., 68(6), 1178–1193, doi:10.1175/2010JAS3694.1, 2011.

Gray, S. L.: Mechanisms of midlatitude cross-tropopause transport using a potential vorticity budget approach, J. Geophys. Res., 111, D17113, doi:10.1029/2005JD006259, 2006.

Kunkel, D., Hoor, P., and Wirth, V.: Can inertia-gravity waves persistently alter the tropopause inversion layer?, Geophysical Research Letters, 41, n/a–n/a, https://doi.org/10.1002/2014GL061970, 2014.

Kunkel, D., Hoor, P., and Wirth, V.: The tropopause inversion layer in baroclinic life-cycle experiments: the role of diabatic processes, Atmospheric Chemistry and Physics, 16, 541–560, https://doi.org/10.5194/acp-16-541-2016, 2016.

Lamarque, J.-F. and Hess, P. G.: Cross-Tropopause Mass Exchange and Potential Vorticity Budget in a Simulated Tropopause Folding, Journal of the Atmospheric Sciences, 51, 2246–2269, https://doi.org/10.1175/1520-0469(1994)051<2246:CTMEAP>2.0.CO;2, 1994.

Madonna, E., Wernli, H., Joos, H. and Martius, O.: Warm Conveyor Belts in the ERA-Interim Dataset (1979–2010). Part I: Climatology and Potential Vorticity Evolution, J. Clim., 27(1), 3–26, doi:10.1175/JCLI-D-12-00720.1, 2014.

Plougonven, R. and Snyder, C.: Gravity waves excited by jets: Propagation versus generation, Geophys. Res. Lett., 32(18), L18802, doi:10.1029/2005GL023730, 2005.

Plougonven, R. and Snyder, C.: Inertia–Gravity Waves Spontaneously Generated by Jets and Fronts. Part I: Different Baroclinic Life Cycles, J. Atmos. Sci., 64, 2502–2520, doi:10.1175/JAS3953.1, 2007.

Plougonven, R. and Zhang, F.: Internal gravity waves from atmospheric jets and fronts, Rev. Geophys., 52, n/a-n/a, doi:10.1002/2012RG000419, 2014.

Spreitzer, E., R. Attinger, M. Boettcher, R. Forbes, H. Wernli, and H. Joos, 2019: Modification of Potential Vorticity near the Tropopause by Nonconservative Processes in the ECMWF Model. J. Atmos. Sci., 76, 1709–1726, https://doi.org/10.1175/JAS-D-18-0295.1

Wei, J. and Zhang, F.: Mesoscale Gravity Waves in Moist Baroclinic Jet–Front Systems, J. Atmos. Sci., 71(3), 929–952, doi:10.1175/JAS-D-13-0171.1, 2014.

Zhang, F., Wei, J., Zhang, M., Bowman, K. P., Pan, L. L., Atlas, E., and Wofsy, S. C.: Aircraft measurements of gravity waves in the upper troposphere and lower stratosphere during the START08 field experiment, Atmos. Chem. Phys., 15, 7667–7684, https://doi.org/10.5194/acp-15-7667-2015, 2015.

Evidence of small-scale quasi-isentropic mixing in ridges of extra-tropical baroclinic waves

Daniel Kunkel[1], Peter Hoor[1], Thorsten Kaluza[1], Jörn Ungermann[2], Björn Kluschat[1], Andreas Giez[3], Hans-Christoph Lachnitt[1], Martin Kaufmann[2,4], and Martin Riese[2,4]

[1]Institute for Atmospheric Physics, Johannes Gutenberg University, Mainz, Germany
[2]IEK-7, Forschungszentrum Jülich, Jülich, Germany
[3]Flight Experiments, Deutsches Zentrum für Luft- und Raumfahrt, Oberpfaffenhofen, Germany
[4]Institute for Atmospheric and Environmental Research, University of Wuppertal, Wuppertal, Germany

Correspondence: Daniel Kunkel (dkunkel@uni-mainz.de)

Abstract. Stratosphere-troposphere exchange within extratropical cyclones provides the potential for anthropogenic and natural surface emissions to rapidly reach the stratosphere as well as for ozone from the stratosphere to penetrate deep into the troposphere, even down into the boundary layer. The efficiency of this process directly influences the surface climate, the chemistry in the stratosphere, the chemical composition of the extratropical transition layer, and surface pollution levels. Here, we present evidence for a mixing process within extratropical cyclones which has gained only little attention so far and which fosters the transport of tropospheric air masses into the stratosphere in ridges of baroclinic waves. We analyzed airborne measurement data from a research flight of the WISE (Wave driven isentropic exchange) campaign over the North Atlantic in autumn 2017 supported by forecasts from a numerical weather prediction model and trajectory calculations. Further detailed process understanding is obtained from experiments of idealized baroclinic life cycles. The major outcome of this analysis is that air masses mix in the region of the tropopause and potentially enter the stratosphere in ridges of baroclinic waves at the anti-cyclonic side of jet without changing their potential temperature drastically. This quasi-isentropic exchange occurs above the outflow of warm conveyor belts, in regions which exhibit enhanced static stability in the lower stratosphere and a Kelvin-Helmholtz instability across the tropopause. The enhanced static stability is related to radiative cooling below the tropopause and the presence of small scale waves. The Kelvin-Helmholtz instability is related to vertical shear of the horizontal wind associated to small scale waves at the upper edge of the jet-stream. The instability leads to the occurrence of turbulence and consequent mixing of trace gases in the tropopause region. While the overall relevance of this process has yet to be assessed, it has the potential to significantly modify the chemical composition of the extratropical transition layer in the lowermost stratosphere in regions which have previously gained only little attention in terms of mixing in baroclinic waves.

1 Introduction

The extratropical transition layer (ExTL) as a unique feature of the extratropical upper troposphere and lower stratosphere (UTLS) is a direct consequence of the exchange and consequent mixing between air masses from the stratosphere and troposphere (e.g., Danielsen, 1968; Gettelman et al., 2011). The depth of this transition layer is commonly diagnosed from vertical distributions of ~~certain trace species with distinct tropospheric and~~ trace species such as CO, O_3, H_2O, or N_2O with either distinct tropospheric or stratospheric sources and from tracer-tracer correlations (e.g., Hoor et al., 2002; Pan et al., 2004). In the northern summer the ExTL extends up to 30 K in potential temperature above the local dynamic tropopause and between 20-25 K in all other seasons (Hoor et al., 2004). In the southern hemisphere, the ExTL seems to be more shallow (Hegglin et al., 2009).

The vertical distribution of trace species in the extratropical UTLS crucially depends on the large scale stratospheric circulation (e.g., Butchart, 2014) and on stratosphere-troposphere exchange (STE) across the tropopause (e.g., Holton et al., 1995; Stohl et al., 2003; Sprenger et al., 2003). Overall, there are three prominent pathways for air into the ExTL. ~~First, the stratospheric circulation~~ The stratospheric circulation contributes with two distinct branches distinguished based on the transit time between the major entry point of air into the stratosphere, i.e., the tropical tropopause, and the extratropics. The so called deep branch, i.e., associated with long transit times affects the ExTL through the descent of old stratospheric ozone rich air ~~in the deep branch~~ into the UTLS. ~~Second,~~ In contrast, the shallow branch with significantly shorter transit times introduces relatively young air from the tropical and subtropical UTLS ~~can enter the region of~~ into the extratropical UTLS ~~through fast two-way eddy mixing in the shallow branch of the stratospheric circulation~~(Birner and Bönisch, 2011). A recent study based on airborne measurements showed the effect of these two ~~competing~~ transport pathways on the changing abundance of carbon monoxide (CO) over the course of the Arctic winter in the ExTL (Krause et al., 2018). A third pathway into the ExTL is direct injection of extratropical tropospheric air into the stratosphere by troposphere-to-stratosphere transport (TST). ~~In the extratropics STE predominantly occurs in association with processes in baroclinic planetary- and synoptic-scale waves (Sprenger et al., 2003, 2007), small scale gravity waves (Langford et al., 1996; Whiteway et al., 2003; Miyazaki et al., 2010), and in regions affected by convective systems (e.g., Poulida et al., 1996; Tang et al., 2011; Homeyer, 2015). Together these processes~~ These pathways all shape the vertical profiles of the trace species ~~and thus~~ across the extratropical tropopause and thus can have an impact on the surface climate trough a radiative feedback mechanism. Changes in the vertical abundance of radiatively active trace species in the UTLS, for instance for water vapor and ozone, relatively have the largest impact on the surface temperature (Riese et al., 2012).

Climatological studies revealed that in the northern hemisphere mid latitudes STE occurs predominantly in regions of enhanced cyclone activity, the storm tracks, over the North Atlantic and Pacific as well as over the Mediterranean Sea (Sprenger et al., 2003). Generally, in the extratropics STE occurs more frequently during winter and more mass is transported from the stratosphere into the troposphere, i.e., stratosphere-to-troposphere transport (STT) than vice versa, i.e., TST. This has recently been reported by Škerlak et al. (2014) who analyzed STE based on a 33 year long time period of ERA-Interim reanalysis data and trajectory calculations. This analysis further confirmed earlier studies with respect to spatial and temporal occurrence of STE (e.g., Chen, 1995; Morgenstern and Carver, 1999; Dethof et al., 2000). ~~These results are~~ Also in a climatological sense the occurrence of STE in the extratropics is independent of the definition of the tropopause as shown by Boothe and Homeyer (2017) who used four different modern reanalysis data sets to analyze STE as well as first lapse-rate (lrt1) and dynamic tropopause definitions.

~~In the extratropics~~ Within the storm tracks Rossby waves are crucial for STE. During their life cycle, Rossby waves can lead to the formation of so called stratospheric streamers and cut-off lows, both being regions of strong STE activity (Sprenger et al., 2007). STE occurs also in tropopause folds along jet streams due to the cross-frontal secondary circulation. Sprenger et al. (2003) demonstrated that exchange between subtropical and extratropical air masses across the subtropical jet predominantly occurs in these folds, but tropopause folds exists also at higher latitudes (Škerlak et al., 2015). Idealized simulations of baroclinic life cycles and analyses of reanalysis data showed that dynamic instabilities with low Richardson numbers, thus large vertical shear of the horizontal wind, lead to mixing around tropopause folds (Bush and Peltier, 1994; Jaeger and Sprenger, 2007). Using similar data and methods as Škerlak et al. (2014), Reutter et al. (2015) studied the relevance of extratropical cyclones for STE over the North Atlantic. They found that the STT mass flux is generally larger than the TST mass flux and that the region of the exchange varies slightly during the life cycle of the cyclone~~but most exchange takes place around the cyclone center in regions with low tropopause~~. This study also confirmed earlier findings which suggested that STE occurs close to the cyclone center or rather in regions with a relatively low tropopause height, thus more on the cyclonic side of the jet in the region of the trough (e.g., Wernli and Davies, 1997).

~~All processes which lead to cross tropopause transport of air parcels have one common impact on this air parcel , they change~~ An air parcel crossing the tropopause has to be affected by non-conservative processes which can modify its potential vorticity ~~(PV). Such PV non-conserving processes must act on~~ (Hoskins et al., 1985). Only then the air parcel ~~and are related to radiation, phase changes of water in the atmosphere, and friction (Hoskins et al., 1985).~~ can enter from a region with generally low PV, i.e., the troposphere, into a region of high PV, i.e., the stratosphere or vice versa. Lamarque and Hess (1994) separated between diabatic, i.e., potential temperature changing, and diffusive, i.e., related to friction, processes and showed that diabatic processes play a more vital role for STE than diffusive processes. Analyzing cross tropopause transport in the UKMO model Gray (2006) found similar results with cloud and radiative processes being more important for STE than processes related to turbulence. In contrast, a recent study by Spreitzer et al. (2019) shows that turbulent processes are mainly responsible for changing the PV around the tropopause in a ridge of an extratropical baroclinic wave. They used high resolution ECMWF forecast data and conclude that turbulence is evident around the jet stream. This turbulence is mainly related to the vertical shear of the jetstream but can also be caused by gravity waves Zhang et al. (2015a). Radiative effects may play an important role in anti-cyclones (Zierl and Wirth, 1997) where radiation lowers the tropopause and thus leads to a mass flux from the troposphere into the stratosphere. Radiation is also a key process to dissolve stratospheric cut-off lows in the troposphere (Forster and Wirth, 2000). Clouds and related diabatic heating may also have an impact on

STE. For instance warm conveyor belts, i.e. airstreams ahead of cold fronts associated with extratropical cyclones in which strong diabatic heating by latent heat release occurs (e.g., Wernli and Davies, 1997), can reach the upper troposphere and modify the PV, consequently allowing for exchange between tropospheric and stratospheric air (Wirth, 1995; Wernli and Bourqui, 2002). According to Spreitzer et al. (2019) clouds change PV rather in regions with lower tropopause altitudes, e.g., in the trough. Similar, rapid transfer from the boundary layer into the UTLS is evident in convective systems, which sometimes have the potential to overshoot into the stratosphere ~~(Poulida et al., 1996; Stenchikov et al., 1996; Homeyer et al., 2014)~~ (e.g., Poulida et al., 1996; Stenchikov et al., 1996; Homeyer et al., 2014; Homeyer, 2015; Tang et al., 2011). Convection can also trigger gravity waves which occasionally break or dissipate and thus lead to small scale mixing between tropospheric and stratospheric air masses ~~(Whiteway et al., 2003)~~(e.g., Whiteway et al., 2003). Jet-induced gravity waves might play a vital role for STE on small scales, inducing turbulence and consequently allow for mixing between adjacent atmospheric layers (e.g., Langford et al., 1996; Lamarque et al., 1996). Strong shear zones are often apparent at the edges of the jet-streams which lead to filamentation of tropospheric or stratospheric air masses (Appenzeller et al., 1996). In these shear zones Kelvin-Helmholtz instabilities can emerge and lead to intense turbulence (e.g., Pepler et al., 1998; Whiteway et al., 2004). In turn this can lead to mixing of air masses around the jet streams. However, this mixing is thought to be more relevant at the lower edge (e.g., Danielsen, 1968; Shapiro, 1980) and on the cyclonic side of the jet, thus rather in the trough than in the ridge of baroclinic waves (e.g., Pan et al., 2007; Konopka and Pan, 2012).

Only a few studies focused on mixing and STE on the anti-cyclonic side of jet in the ridges of baroclinic waves. Early suggestion were based on individual airborne observations with small scale waves being responsible for cross tropopause transport in these regions (Shapiro, 1980; Danielsen et al., 1991). Model simulations by Lamarque and Hess (1994) showed that PV is not conserved in the ridge of the studied baroclinic wave and that cloud related processes lead to STE. Forster and Wirth (2000) showed how radiative effects can affect the tropopause altitude in anti-cyclones and thus lead to mass exchange from the troposphere into the stratosphere over the course of several days. Recently, Kunkel et al. (2016) showed that turbulent motions can occur on top of warm conveyor belt outflows at the altitude of the tropopause. This coincidence of turbulence in a region of the so called tropopause inversion layer ~~(TIL, Birner et al., 2002)~~ (TIL, Birner et al., 2002) addresses an open question in the extratropical UTLS which is in particular relevant for the ExTL: ~~Does the TIL~~ Does STE occur and does it affect the formation of the ExTL ~~by inhibiting mixing or STE?~~ in the ridge of baroclinic waves where the static stability is usually strong in the extratropical lowermost stratosphere?

This study picks up the idea of turbulent mixing in regions of enhanced lower stratospheric static stability which ~~initial~~ initially resulted from experiments of baroclinic life cycles (Kunkel et al., 2016) and which has recently been described by ~~Kaluza et al. (2018)~~ Kaluza et al. (2019) in composites of baroclinic waves over the North Atlantic. Birner et al. (2002) and Grise et al. (2010) both discussed that enhanced values of static stability and shear zones emerge in close vicinity at the tropopause level. Zhang et al. (2015b) addressed this further by linking the enhanced wind shear to propagating inertia-gravity waves with the potential to induce mixing, however, without addressing the larger scale meteorological conditions explicitly.

In this study we aim to analyze whether those turbulent signatures lead to mixing and potential exchange of tropospheric and stratospheric air masses in the ridge of baroclinic waves. For this we use complementary data of airborne measurements, numerical weather forecast data, trajectory calculations, and idealized baroclinic life cycle experiments which are introduced in Section 2. We will first focus on a research flight from the Wave-Driven Isentropic Exchange campaign (Section 3) which aimed to measure chemical constituents and state parameters across the tropopause in a baroclinic wave over the North Atlantic. We then extend a set of well known idealized simulations of baroclinic life cycles to analyze STE and to obtain a comprehensive understanding of the processes which lead to mixing and potential STE in the ridge ~~of the baroclinic waves~~ (Section 4). We finalize our study with a summary and a conclusion in Section 5.

2 Data and methods

2.1 Measurements during the WISE campaign 2017

In autumn 2017 the airborne research mission Wave-driven ISentropic Exchange (WISE) took place from Oberpfaffenhofen, Germany and Shannon, Ireland with the German HALO (High Altitude Long range) research aircraft. The main goals of the mission ~~are~~ were to examine mixing processes in the UTLS in association with Rossby wave breaking and to study the impact of the Asian Summer Monsoon circulation on the budget of radiatively active species in the lower stratosphere. One specific target ~~is~~ was to study the relation between the lower stratospheric static stability and cross-tropopause exchange in the extratropics.

During WISE HALO was equipped with a unique set of instruments for in-situ and remote sensing measurements. In this study we use in-situ measurements of CO and N_2O, and potential temperature Θ. CO and N_2O have been measured with the University of Mainz Airborne Quantum Cascade Laser Spectrometer (UMAQS). The instrument is based on direct absorption spectroscopy using a continuous-wave quantum cascade laser with a sweep rate of 2 kHz (Müller et al., 2015). For the WISE campaign the total drift-corrected uncertainty were determined to be $0.94\,\mathrm{ppb_v}$ for CO and $0.18\,\mathrm{ppb_v}$ for N_2O. Basic state parameters such as temperature, pressure, the three-dimensional wind vector and others ~~are~~ were measured with Basic HALO Measurement and Sensor System (BAHAMAS). The system is part of the basic aircraft and consists of a data acquisition system and a suite of sensors for basic meteorological and aerodynamic measurements. The system also contains interfaces into several aircraft systems like the inertial reference unit or the air data computer in order to monitor aircraft state parameters (Krautstrunk and Giez, 2012). The nose boom of HALO is part of ~~the~~ this system and carries the air data probe for pressure and air flow measurements which are needed for determination of the wind vector. Additional BAHAMAS installations are six Total Air Temperature (TAT) housings on the aircraft nose which can be used for temperature measurements and as inlets for sensors inside the nose. Two of these housings contain an open wire PT100 resistance thermometer for atmospheric temperature measurements thus providing redundancy for this important parameter. The basic frequency for all atmospheric units is 100 Hz, data is usually processed on a 10 Hz basis. The accuracy of the pressure measurement is 0.3 hPa while the accuracy of the static temperature measurement is 0.5 K. We also ~~will show~~ use remote sensing measurements from the Gimballed Limb Observer for Radiance Imaging of the Atmosphere (GLORIA), which provides profile information of temperature and static stability, in addition to numerous trace gases (not used in this study). GLORIA is an airborne infrared limb imager combining a two-dimensional infrared detector with a Fourier transform spectrometer (Friedl-Vallon et al., 2014; Riese et al., 2014). The viewing direction is to the right of flight direction and depending on flight altitude and flight direction GLORIA observes the atmosphere between about 5 km and flight altitude with a vertical sampling of about 150 m at a tangent altitude of 10 km. The vertical resolution of retrieved temperature profiles and static stability is of the order of 300 m. The horizontal sampling along the flight track is up to 2 km (Kaufmann et al., 2015; Ungermann et al., 2015).

In total the WISE campaign comprised more than 140 flight hours during 15 research flights between 12.09.2017 and 21.10.2017. All flights except the first two started in Shannon, Ireland and covered the North Atlantic between Greenland, Newfoundland, the Azores, and Europe as well as continental Western and Northern Europe. HALO was mostly flying in the UTLS up to ceiling altitudes of about 15 km, which corresponds to maximum potential temperature values of about 405 K and minimum pressure values of 130 hPa. ~~Research~~ The goal of research flight 07 (RF07) on 28.09.2017 ~~had the goal~~ was to study the abundance of trace species in the extratropical tropopause region~~in relation to the occurrence~~. In particular, in accordance to the major goals of the WISE mission, the focus of this flight was on whether the trace species show specific signs of recent STE in regions of enhanced values of static stability in the lower stratosphere~~and to potential STE. Such conditions in the ridge of extratropical baroclinic waves resemble~~. Furthermore, the design of this flight was chosen such that the predictions of the idealized simulations ~~from Kunkel et al. (2016)~~ of Kunkel et al. (2016) could be supported by observations. Thus, the flight was planned in the ridge of a synoptic-scale baroclinic wave which evolved during the previous days over the North Atlantic at the edge of a larger scale trough. A detailed description of the synoptic situation and the flight path will be given in Sec. 3.1.

2.2 ECMWF forecast data

We use forecast data from the European Centre for Medium-Range Weather ~~Forecast~~ Forecasts (ECMWF) to support the analysis of the airborne measurements and to provide more background information about the synoptic situation. We choose to use forecast data from ECMWF because it is hourly available at a very fine horizontal resolution. The forecast starts at 28.09.2017 00 UTC and we use the first 36 hourly steps until 29.09.2017 12 UTC. This data is used for analysis along the flight path where the full resolution is used corresponding to regular longitude/latitude grid spacing of about $0.07°$. Moreover, we use a slightly degraded data set with a horizontal grid spacing of $0.125°$ in the horizontal for a trajectory analysis. The forecast data has 137 vertical hybrid pressure-sigma levels up to 0.01 hPa with a vertical spacing of roughly 300 m in the UTLS.

2.3 Idealized baroclinic life cycle experiments

We complement our analysis of the airborne measurements using results from idealized baroclinic life cycle experiments. We continue the work of Kunkel et al. (2016) using the same setup of the COSMO model ~~(Steppeler et al., 2003)~~ (COnsortium for Small-scale MOdelling, Steppeler et al., 2003) but extend the analysis with a more specific focus to analyze STE. For this we included additional artificial tracers to mark air masses which are initially located either in the troposphere or in the stratosphere, separated by the dynamic tropopause for which we use the isosurface of 2 pvu ($1\,\mathrm{pvu} = 10^{-6}\,\mathrm{K\,m^2\,kg^{-1}\,s^{-1}}$).

Moreover, we included a tracer which is passively advected and which carries the information of the initial value of potential vorticity. With this tracer it is possible to determine how much PV in each model box has changed by diabatic processes since model start (Kunkel et al., 2014). Evaluating the difference between the current PV and the advected initial PV at the dynamic tropopause allows then to detect regions of TST and STT.

We then repeated simulations from Kunkel et al. (2016) which included parameterizations for large scale and convective clouds, radiation and turbulence which have been labeled with BRTC (BRTC = Bulk microphysics, Radiation, Turbulence, and Convection) by these authors. The model grid has a regular horizontal grid spacing of $0.4°$ in longitude and latitude and a vertical grid spacing of 110 m in the UTLS. Since the meteorological situation during RF07 was dominated by wave breaking event strongly resembling a life cycle 1 (LC1), we will focus our discussion in Section 4 to results from LC1 experiments (Thorncroft et al., 1993), but we note that we also conducted simulations of life cycle 2 (LC2). Moreover, the LC2 experiments qualitatively gave the same results as the LC1 experiments. More information about the model setup and physics is given in ~~Kunkel et al. (2016) and references therein~~Appendix A.

2.4 Trajectory calculations with LAGRANTO

The LAGrangian ANalysis TOol LAGRANTO (Sprenger and Wernli, 2015) allows calculating trajectories using the kinematic wind from four dimensional meteorological data. It is possible to use both ECMWF and COSMO data as input for the trajectory calculations. The first trajectory analysis is based on ECMWF forecast data which provides wind fields every hour. Trajectories have been initialized along the flight path with the goal to obtain a more comprehensive picture of the temporal evolution of meteorological parameters of the measured air masses. We will give more details on the trajectory start points and the analysis in Section 3.3.

For the second trajectory analysis we use COSMO wind fields. COSMO output is available every hour on a horizontal grid with spacing of $0.4°$ and a vertical spacing of about 110 m in the UTLS, thus providing a high resolution input grid for the trajectory calculations. Based on the COSMO model output the goal of the trajectory calculations is to identify regions of cross tropopause transport in the baroclinic life cycle experiments and whether exchange trajectories are evident in the ridge of the baroclinic wave. More details will be given in Section 4.

In general, we identify the exchange of air masses between the stratosphere and troposphere by the evolution of ~~the~~ PV along a trajectory. ~~In this study we use the 2 pvu isosurface as dynamic tropopause.~~ If the PV of an air parcel increases from values below 2 pvu to values above this threshold, we mark this trajectory as a TST-trajectory and vice versa for STT.

Finally, note that in this study discussion around static stability are usually associated with the first lapse rate tropopause, while discussion about STE are linked to the dynamic tropopause. Thus, both definitions will be considered in the analysis.

however, if only the term tropopause is used, then we refer to the dynamic tropopause with a value of 2 pvu throughout the manuscript.

3 Quasi-isentropic mixing in a ridge of a baroclinic wave during WISE

3.1 Synoptic situation and flight plan of WISE RF07

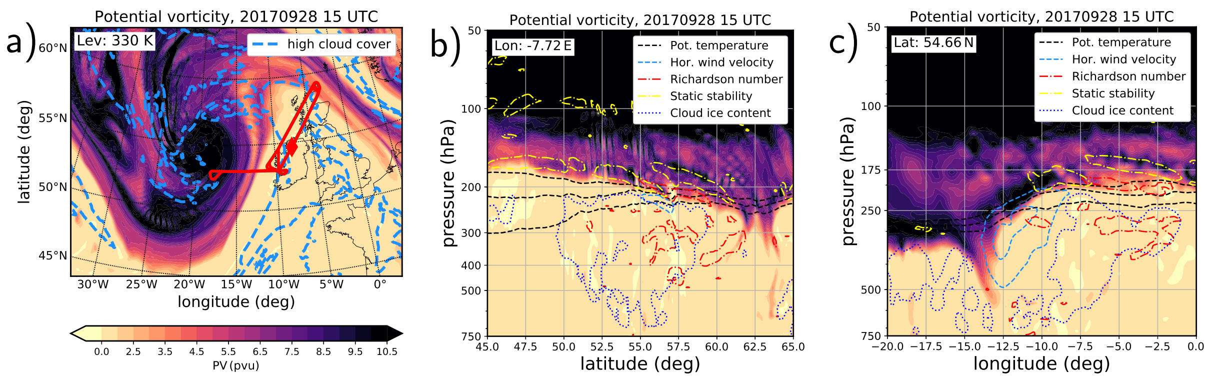

Figure 1. Synoptic situation during WISE RF7 over the Western North Atlantic at 15 UTC on 28.09.2017. ~~Left panels show potential vorticity~~ a) Potential vorticity on the isentropic surface ~~with~~ of 330 K with high cloud cover (~~blue dashed marks~~ isoline showing a value of 0.9)~~, e~~. b) Meridional cross section of potential vorticity along $-7.72\,^{\circ}$E longitude ~~,~~and ~~e~~c) zonal cross section along $54.66\,^{\circ}$N latitude. ~~Panels c) and e) include~~ The cross sections also show isolines of potential temperature (black ~~, values of~~ dashed; 330 K, 335 K, 340 K), of horizontal wind velocity (light blue ~~, values of 35 ms^{-1},~~ dashed; 45 ms^{-1}, 55 ms^{-1}~~, and 65 ms^{-1}~~), ~~and of~~ the Richardson number (red ~~, value of 1.0~~dash-dotted; 1)~~. Right panels show~~, static stability (~~in 10^{-4} s^{-2}) b~~yellow dash-dotted; 5.5×10^{-4} s^{-2})~~as the mean value between the local thermal tropopause~~ , and ~~1 km above with integrated~~ cloud ice ~~column between 1.5 km below the local thermal tropopause, i.e., the first lapse-rate tropopause (lrt1) and this level~~ content (blue ~~dashed, value of 2.5×10^{-3} kg m^{-2}~~dotted; 5×10^{-6} kg kg^{-1}). ~~Panels d) and f) show~~ The cross sections ~~of static stability accordingly to panels c)~~ are along the meridian and ~~e) with isolines showing cloud water content (black, values~~ the circle of ~~5×10^{-6} kg kg^{-1}), cloud ice content (blue, values~~ latitude of ~~5×10^{-6} kg kg^{-1}), and~~ the ~~Richardson number (~~red ~~, value of 1.0~~diamond shown in panel a). ~~The first lapse-rate tropopause~~ This point also marks the location where the picture in Figure 2b is ~~defined following WMO (1957)~~taken.

WISE RF07 targeted a fast evolving baroclinic wave which emerged at the southern tip of a large scale trough in the central North Atlantic in the early hours of 27.09.2017. While the large scale trough traveled relatively slow over the North Atlantic, the small scale wave evolved rather fast, with a formation of a warm sector and well defined upper tropospheric fronts within 24 hours as indicated by the PV at 330 K at 15:00 UTC on 28.09.2017 (Figure 1a).

The flight focused on the rapidly evolving ridge, which was expected to be strongly affected by diabatic processes and vertical transport of boundary layer air in region of the warm conveyor belt (WCB) ahead the surface cold front. This system was

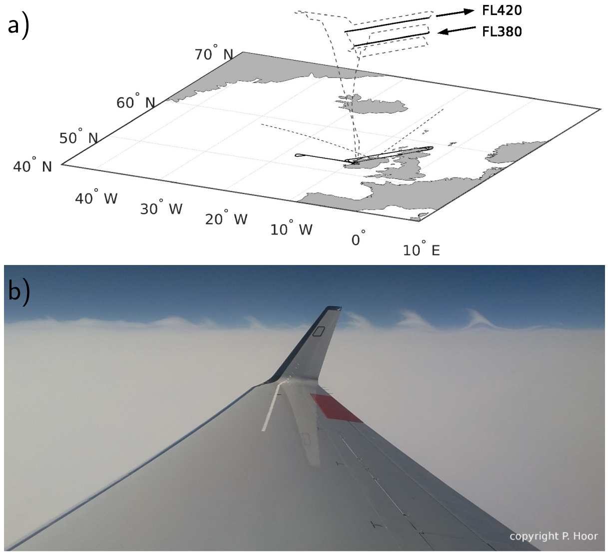

Figure 2. a) Three dimensional flight track of WISE RF07, ~~color-coded with pressure (~~highlighting the flight legs important for this study. The arrows point in ~~hPa) and~~ the direction of the flight on the respective levels. The dashed lines on the surface map show the angle of view of the photo shown in b~~) indicated by the dashed lines on the surface~~. b) Photo taken on board HALO at 15:03 UTC during WISE RF07 showing Kelvin-Helmholtz cloud billows on top of a cirrus cloud deck.

expected to be situated close to Ireland in the afternoon hours of 28.09.2017. Take-off of WISE RF07 was at 13.15 UTC with a total flight time of 7h 47min. The flight strategy was twofold: first stagged flight levels at FL400 (north-eastward), FL380 (south-westward), FL360 (north-eastward), FL340 (south-westward), FL420 (north-eastward), and FL450 (south-westward) through the ridge of the baroclinic wave and second a survey of the stratospheric air with large PV values above the occlusion of the baroclinic wave west of Ireland (see also flight path in Figures 1a ~~,b~~ and 2a). The intention of the first part in the northernmost part of the ridge of the baroclinic wave was to conduct co-located measurements of atmospheric state parameters and trace species across the local tropopause. The stagged flight level allowed to measure these quantities in-situ at different altitudes below, at, and above the level of the tropopause. From the highest flight levels (FL420 and FL450) in cloud-free conditions two dimensional distributions of temperature and trace species along the flight track were remotely measured with GLORIA. Our analysis focuses on the first part of the RF07, in particular on the first flight leg in south-westward direction at FL380 (see Figure 2a).

A large part of the first leg at FL380 in south-westerly direction was close above a wide-spread cirrus cloud deck associated with the upper tropospheric outflow of the WCB of the low pressure system. The high cloud cover in Figure 1a shows the location of this cloud deck. The WCB manifests also in the low values of PV in the upper troposphere in the region where the ice clouds reach up to the tropopause (Figures 1~~c,d~~b,c). PV values are close to 0 pvu or even slightly below which is common in such a situation due to a decreasing heating rate above the level of maximum heating (e.g., Chagnon et al., 2013; Joos and

Wernli, 2012).

~~The~~ In the lower stratosphere the PV shows enhanced variability above the WCB outflow region ~~in the lower stratosphere~~ (Figures 1~~c,e). These structures are even more evident in static stability (Figures 1d,f). Maximum values are above $10 \times 10^{-4}\,\mathrm{s}^{-2}$ with almost tropospheric background values in between. Kunkel et al. (2016) linked these large values of static stability to moist tropospheric dynamics related to the WCB ascent and to the radiative feedback from cirrus clouds close to the (thermal) tropopause. Additional contributions might result from propagating inertia-gravity wave in the lowermost stratosphere (Kunkel et al., 2014). In parts of the regions of enhanced static stability in the lowermost stratosphere low Richardson numbers emerge with values below 1. These low values suggest the potential occurrence of turbulent motions in the region of the tropopause.~~ b,c). There are also high values of static stability evident with values reaching as high as $10 \times 10^{-4}\,\mathrm{s}^{-2}$. However, these high values emerge rather as wave like patches and not as a layer. In between the high values the static stability has rather tropospheric background values (see also Figure 3). More so, this region also exhibits low values of the Richardson number, indicative for Kelvin-Helmholtz instability and thus turbulence. Such a co-located enhancement of static stability and presence of turbulence was also evident in the life cycle experiments of Kunkel et al. (2016) and has recently been reported by ~~Kaluza et al. (2018)~~ Kaluza et al. (2019) based on a composite analysis of baroclinic waves over the North Atlantic.

Another indication of turbulence in the region above the cloud deck stems directly from observations of Kelvin-Helmholtz cloud billows close to the flight path (Figure 2b). A photo was taken at 15.03 UTC in a north-western direction (Figure 2a, diamond in Figures 1a,b). The billows are indicative for a Kelvin-Helmholtz instability (KHI) which is thought to favor mixing of adjacent atmospheric layers and thus affects the vertical gradient of trace species. Notably, since the KHI emerges in the vicinity of the tropopause, it could potentially lead to STE. Commonly, a critical Richardson number of 0.25 identifies a KHI. However, in a non-convective situation such small Richardson numbers rely on large vertical shear of the horizontal wind. In turn, models based on a discretized grid with ~~grid spacings~~ a grid spacing of a few hundred meters or more in the vertical can often not resolve the vertical shear sufficiently. In the region of the observed cloud billows we find Richardson numbers in the ECMWF model of about 1. We therefore use a Richardson number equal 1 as a proxy for KHI in the UTLS for our analysis.

Now we focus on the flight leg from north-east to south-west at FL380 between 14.20 and 15.20 UTC. HALO came from FL400 which was then deeper in the stratosphere with potential temperatures above 350 K. At FL 380 HALO was initially flying in the lowermost stratosphere, then gradually approaching and ~~eventually~~ finally crossing the dynamic tropopause ~~horizontally slightly above the dynamic tropopause~~ which was slightly tilted according to the ECMWF analysis (Figure 3a). This is in remarkable agreement with measurements of N_2O, which increases to tropospheric values on FL 380 (Figure 4) as discussed further below. On this leg the aircraft crossed the lower part of the structures with alternating large and low values of static stability. This structure is potentially linked to a propagating inertia-gravity wave which commonly ~~occur~~ emerge during baroclinic wave developments (e.g., O'Sullivan and Dunkerton, 1995). Furthermore, in the region with low values of static stability an area with low Richardson numbers is evident which extends into the region of the maximum of static stability

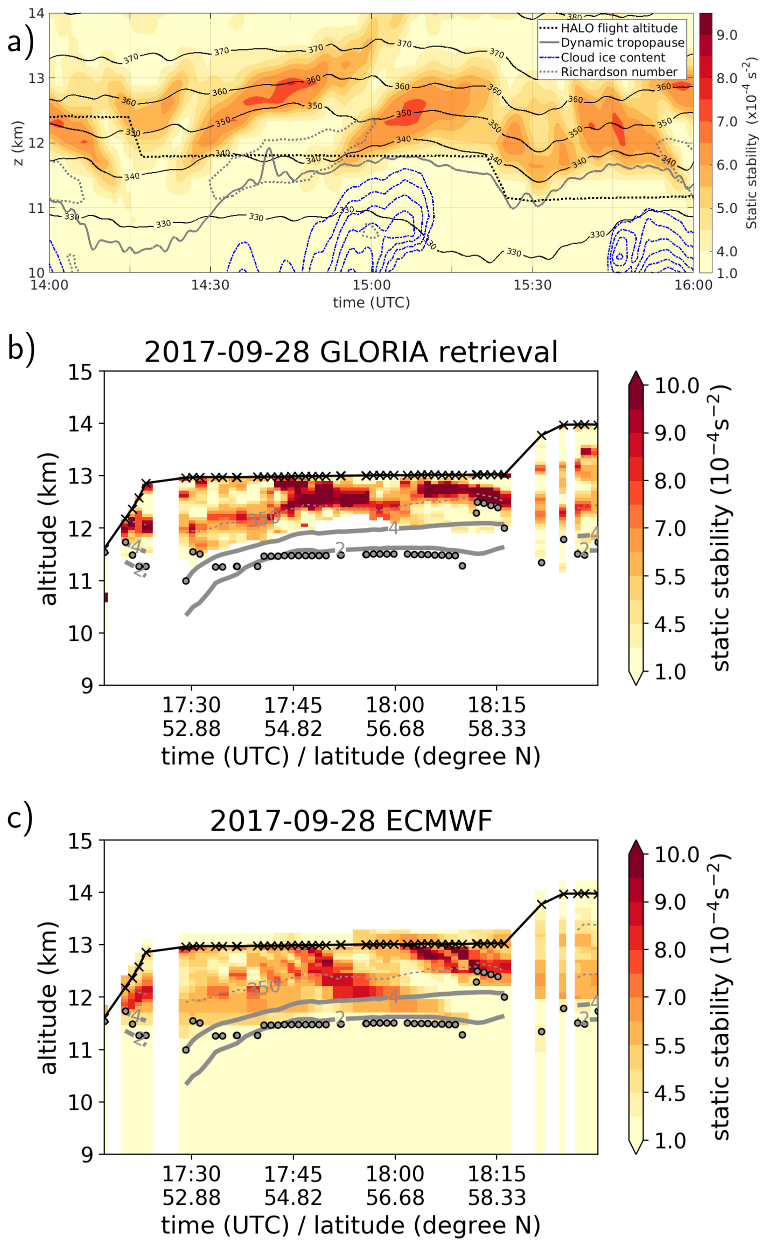

Figure 3. a) Static stability along the flight path between 14:00-16:00 UTC (color-shaded) along with potential temperature (black solid), cloud ice water content (blue dashed), the altitude of the dynamic tropopause (gray solid) and the Richardson number smaller than 1 (gray dotted) based on ECMWF forecast data. Black dotted line shows the altitude of HALO. b) Static stability at GLORIA tangent points between 17:20-18:20 UTC. Black line shows the flight altitude with black crosses marking points of measurement. Thick gray line show 2 and 4 pvu, thin gray line the 350 K isentrope based on ECMWF forecast data. ~~Grey~~ Gray dotted points mark the location of the first lapse rate tropopause. c) ECMWF forecast data sampled at GLORIA tangent points.

around 15 UTC.

Before we analyze the time period between 14:00 and 15:00 UTC more specifically in Section 3.2, we want to point out one model deficiency. Although the ECMWF forecast predicted the atmospheric state very well, there is evidence that extreme values of state parameters are missed or at least underestimated with potential consequences on the representation of mixing in the UTLS. We already mentioned that we think that the Richardson numbers from the ECMWF forecast might have too large values in ~~some~~ regions around the tropopause ~~,~~ where the vertical shear of the horizontal wind is large. However, this is difficult to verify from airborne measurements, since the full two dimensional information on the temperature and wind are missing along the flight path. ~~However,~~ We can overcome this issue at least partly by using temperature retrievals from GLORIA ~~, we can at least~~ and compare static stability (the numerator of the Richardson number calculation) from the model and from measurements (Figure 3b,c). For this we use the last north-eastward leg on FL420, i.e., $\sim$ 13 km and 169 hPa, between 17:20 and 18:20 UTC, when HALO was flying above the maximum values of static stability. Static stability from GLORIA measurements exhibits larger values than from the ECMWF model as well as a smaller vertical extension of the entire wave structure. Thus, the model forecast underestimates the strength of the inversion, most potentially ~~due to defincies~~ related to deficiencies in representing the gravity wave in this region due to the still relatively coarse grid spacing in the UTLS. Since the gravity wave also affects the three dimensional wind, it could be assumed that the vertical shear of the horizontal wind might not be sufficiently represented in the model and thus the Gradient Richardson number.

In summary, the synoptic situation during WISE RF07 strongly resembles the situation of the idealized baroclinic wave of Kunkel et al. (2016). Consequently, it is now possible to investigate a prediction from an idealized model study with airborne measurements and seek ~~for~~ signs of turbulent motions in the measurement data.

3.2 Airborne in-situ measurements and evidence of mixing around the tropopause - WISE RF07

We start our analysis by focusing on the time period between 14:20-14:54 UTC (gray areas in Figure 4) and will first concentrate on the in-situ measurements of nitrous oxide N_2O and potential temperature Θ along with several parameters from the ECMWF forecast interpolated on the flight track. Based on N_2O and Θ we further subdivided the time period of interest into three shorter periods (gray scales in Figure 4). During the first period from 14:20-14:46 UTC N_2O volume mixing ratios below $331.31 \pm 0.45\,\mathrm{ppb_v}$ indicate that HALO was flying in an airmass of stratospheric origin. This value represents the airborne measured tropospheric mean of N_2O during the WISE campaign and is calculated following Müller et al. (2015). HALO was flying at a constant pressure level while slowly approaching the dynamic as well as the first lapse rate tropopause. In the second time period between 14:36-14:48 UTC the distance between tropopause and flight level decreased to a few hundred meters or less according to the PV analysis. Notably, this part of the flight close to the tropopause in the ExTL shows low Richardson numbers. Around 14:40 UTC the time series of both N_2O and Θ show strong wave-like structures with periods of about 2 minutes. The horizontal wavelength can be roughly estimated to be about 25 km, using a mean ground speed of 210 $\mathrm{ms^{-1}}$ of HALO during this part of the flight and assuming that the wave has been crossed perpendicular to the wave crests. The amplitude of the wave is about 2.5 K and the wave spans the potential temperature range between 335-340 K. Interestingly, this wave structure is hardly evident in the modeled Θ_{M}, indicating that the model might have issues representing these scales accurately. The model shows signs of gravity wave activity, however, not directly at the flight altitude but slightly above (not shown). The ECMWF forecast model with a horizontal grid spacing of about 8 km can barely resolve this wave pattern with this fine scale structure due to the grid spacing of the model. The last period between 14:48-14:54 UTC shows a strong variability in both N_2O and Θ without any clear wave signal but a large variability of Θ and N_2O . This increase in variability could be regarded as a first indicator of increased atmospheric turbulence.

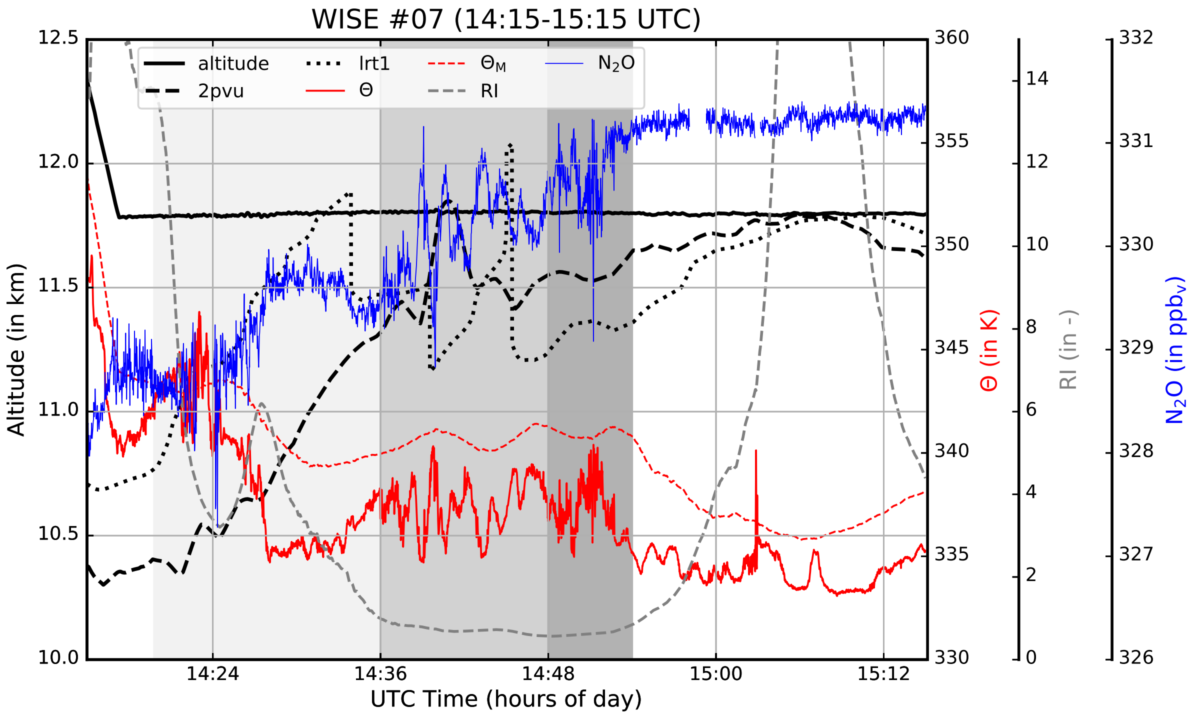

Figure 4. Time series of measured N_2O (blue) and potential temperature ~~Θ_{M}~~ Θ (red solid) as well as modeled potential temperature ~~Θ~~ Θ_{M} (red dashed), Richardson number RI (gray dashed), and ~~altitude~~ altitudes of the dynamic ~~tropopause~~ (2 pvu, black dashed) and the first lapse rate (lrt1, black dotted) tropopause between 14:15 and 15:15 UTC during WISE RF07. Black solid line shows the altitude of the aircraft, the gray areas indicate the time periods discussed in the text.

If turbulence occurred in a region of strong tracer gradients at or upwind of the measurements, it should have affected the composition of trace gases. Both CO and N_2O exhibit vertical gradients in the lower stratosphere (Figure 5a for CO). We first focus on CO since it has a much stronger gradient at the tropopause due to its shorter life time compared to N_2O. HALO was initially in the stratosphere with low values of CO and at the end of the time period close to the troposphere with larger values of CO (Figure 5b). The gradual transition between the more stratospheric to more tropospheric CO values occurs at potential

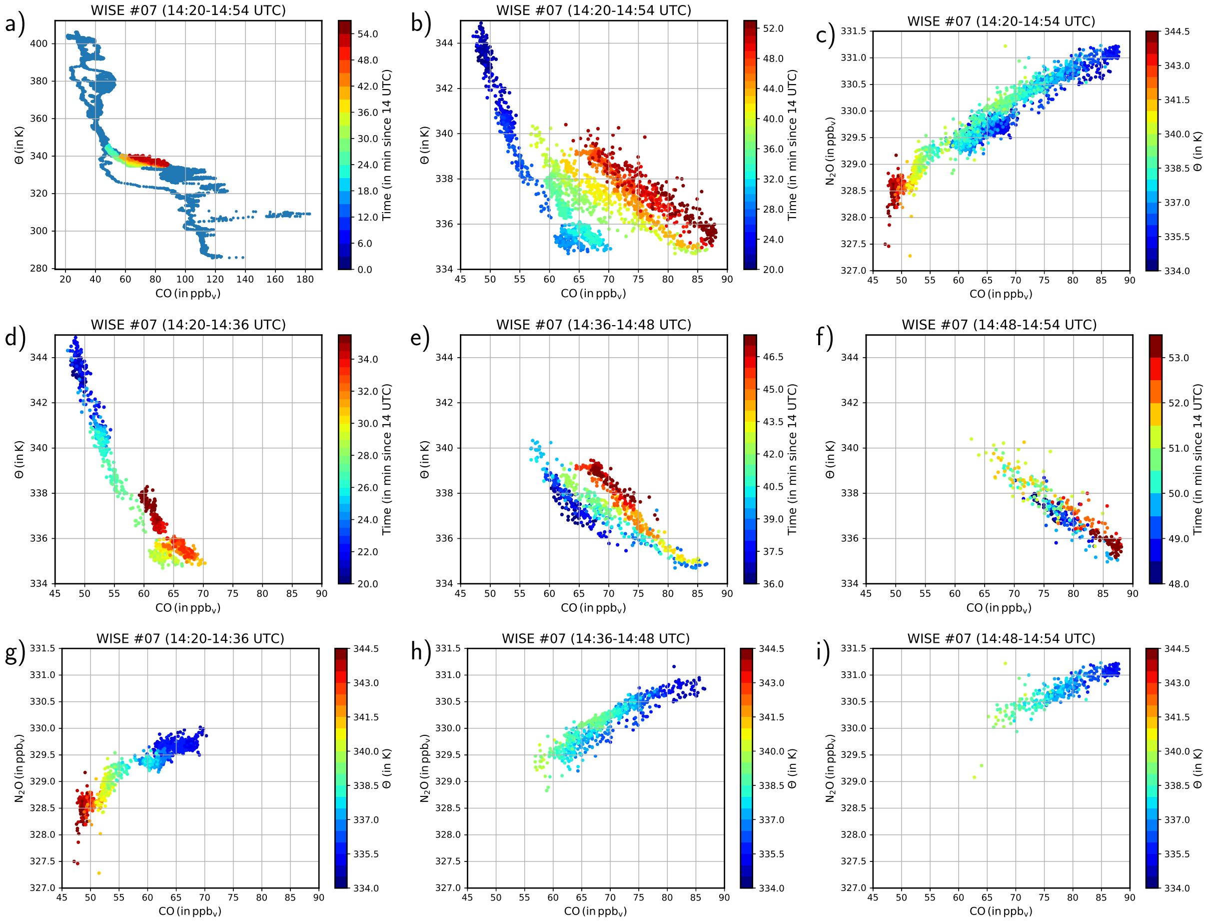

Figure 5. Trace gas analysis of the first south-westward leg on FL380, ~~ie~~i.e. 205 hPa of WISE RF07. a) Vertical profile of carbon monoxide for the entire flight (blue dots) and color-coded for the leg on FL380. b) Vertical profile of CO for the time period between 14:20-15:00 UTC, color-coded with time since 14:00 UTC. c) CO – N_2O correlation for the time period 14:20-15:00 UTC, color-coded with potential temperature. d-f) Vertical profiles of CO for time periods between 14:20-14:36 UTC, 14:36-14:48 UTC, and 14:48-14:54 UTC, color-coded with time. g-i) CO – N_2O correlations for the time periods between 14:20-14:36 UTC, 14:36-14:48 UTC, and 14:48-14:54 UTC, color-coded with potential temperature.

temperatures between 335-340 K. This Θ interval also shows low Richardson numbers in the ECMWF model (Figures 4, 3a). Moreover, the color code in Figure 5b reveals the consecutive alternation between low potential temperature/large CO values and high potential temperature/low CO values, indicating the impact of the small scale wave on the tracer and potential temperature. To identify mixing of tracers, we analyzed the N_2O-CO relationship, which provides information on irreversible tracer exchange similar as CO-O_3 (e.g., Fischer et al., 2000). In general, at the tropopause the $CO-N_2O$ correlation ~~starts with larger~~ shows almost tropospheric mixing ratios of CO ~~and larger~~ ($\sim 90\,\mathrm{ppb_v}$) and N_2O ~~mixing ratios at potential temperatures~~ ($\sim 331\,\mathrm{ppb_v}$) at potential temperature levels typical for the extratropical tropopause ~~,~~ in the current case ($\sim 335\,\mathrm{K}$). Above the tropopause with increasing potential temperature both N_2O and CO mixing ratios decrease. However, the $CO-N_2O$ correlation of the time period between 14:20-14:54 UTC does not show such a clear relationship of decreasing N_2O and CO and simultaneous increasing potential temperature (Figure 5c). If the time period is instead divided into three shorter time periods following the gray shading in Figure 4, then only the first period shows a relationship between N_2O, CO and potential temperature as one would expect from the large scale vertical profiles of these quantities (Figure 5d,g). However, for the other two time periods the tracer-tracer relation with respect to potential temperature changes. For the time between 14:36-14:48 UTC the vertical profile of CO shows a wave-like transition (Figure 5e), while the correlation shows isentropic mixing on different isentropes as indicated by mixing lines connecting tropospheric and stratospheric values between 335-340 K (Figure 5h). In the last time period the relation between N_2O, CO, and potential temperature seems to almost entirely break down, reflecting the initial thought of increased variability in the tracer mixing ratio and potential temperature (Figures 5f,i). Thus, based on the trace gas analysis, we think that turbulence increasingly affected the second and third time periods to a substantial degree in contrast to the first time period. This could ultimately lead to exchange of trace constituents across the tropopause in a narrow range of potential temperature levels.

We further analyze the occurrence of turbulence with the help of power spectral densities (PSD) of potential temperature. Power spectral densities of trace species or state parameters allows to estimate how much energy is present at a particular spatial scale (Vallis, 2017). On board HALO the frequency of measurements is about 10 Hz for the state parameters such as temperature and wind, while it is about 2-3 Hz for CO and N_2O~~, which allows to identify~~. Along with an average ground speed of about 210 $\mathrm{ms^{-1}}$ and with the 10 Hz measurements of the state parameters this potentially allows us to identify atmospheric structures down to about 100 m. The shape of these power spectral densities allows to assess the contribution of individual scale ranges to the total energy spectrum and indicates the type of turbulence that affects the considered domain (Vallis, 2017). The power spectral density from the flight leg on FL380 (Figure 6a) reveals a slope close to $k=-5/3$. This slope often characterizes 3D isotropic turbulence, i.e., dynamic processes on or below the ~~meso scale~~ meso-scale affect the flow ~~(Tung and Orlando, 2003)~~(e.g., Tung and Orlando, 2003; Zhang et al., 2015a). At a later leg in the same direction of the flight on flight level FL420 between 17:20-18:20 UTC the power spectral density follows rather a slope of $k=-3$ (Figure 6b). This slope rather indicates a dominance of geostrophic turbulence and thus larger synoptic scales affecting the flow. ~~Hence, this~~ Summarizing, close to the tropopause the slope of $k=-5/3$ suggests that meso-scale processes, e.g., related to gravity waves, might be substantial to explain the dynamics in the tropopause region.

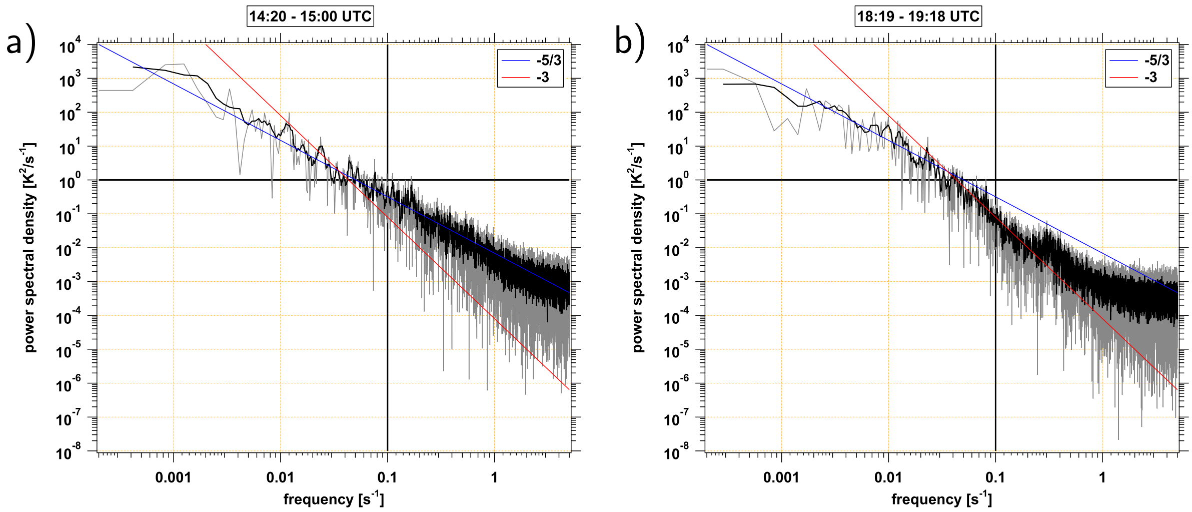

Figure 6. Power spectral densities of measured potential temperature from HALO for selected time periods: a) 14:20 - 15:00 UTC and b) 18:19 - 19:18 UTC. Black solid lines are introduced for better comparability, red solid lines shows a line with a slope of $k = -3$, blue solid line shows a line with a slop of $k = -5/3$.

3.3 Trajectory based history of measured air masses during WISE RF07

The analyses of trace gas distributions, tracer-tracer correlations, and power spectral densities suggest that mixing is evident in the region between 335K and 340 K. In particular, the N_2O mixing ratios reveal that tropospheric and stratospheric air masses participate in mixing process. Our next goal is to elucidate the recent history of the measured air masses. For this we calculated kinematic trajectories back and forward in time which start each second along the flight path for the time period between 14:24 UTC to 14:54 UTC based on ECMWF forecast data available between 28.09.2017 00 UTC and 29.09.2017 12 UTC. More specifically, the trajectories start at the horizontal location of the airplane plus at adjacent locations $\pm 0.07°$ in longitudinal and latitudinal directions to cover some of the uncertainty due to the gridded representation of the meteorological input variables and to increase the number of trajectories for statistical purposes. Moreover, trajectories start at each full isentropic level between 334 K and 341 K and not only at the flight altitude of HALO. This allows us to study the fate of the entire region which is subject to mixing according to the measurement.

Since we are interested in STE and mixing, we first search for those air masses which cross the tropopause around the time of the measurement and which encounter a KHI. For this we filter all trajectories to find those trajectories which cross the dynamic tropopause and which ~~have~~ encounter Richardson numbers smaller than 1 at ~~some time~~ any point in time during the period of the trajectory calculation. We note, however, that our STE criterion is rather weak, since we only require that the PV of the trajectories is below the PV threshold for the dynamic tropopause at the start of the analysis (28.09.2017 ~~00~~ 01 UTC) and above the threshold at the end (29.09.2017 ~~12~~ 11 UTC). Thus, ~~we do not speak~~ for further discussion we rather omit the terminology of TST and STT trajectories in a ~~classical meaning (Stohl et al., 2003).~~ sense of coherent ensembles of trajectories which cross the tropopause only once from the troposphere (stratosphere) to the stratosphere (troposphere) (Stohl et al., 2003; Wernli and Davies, 1997). We rather think of trajectories which show the potential of mixing around the tropopause by encountering low Richardson numbers and having PV values changing between tropospheric and stratospheric values, nevertheless leading to a subsequent exchange across the tropopause. As mentioned above, we consider low Richardson numbers in the order of one as good proxies for KHI. We further study the three time periods of interest from the earlier analysis separately (Figure 4).

Interestingly, we find trajectories indicating upward transport which show the same ~~behaviour~~ behavior in dynamic and thermodynamic quantities in each of the three time periods between 14:20 UTC and 14:54 UTC. These trajectories always follow a wave like flow from the North Atlantic towards the British Islands before they turn anti-cyclonically towards central Europe (Figure 7). Minimum pressure is evident over the North Atlantic when the trajectories pass through the large scale trough. Over Ireland and the British Islands the trajectories rise again while encountering the region of the KHI with minimum Richardson numbers. Starting from this region the trajectories strongly decelerate (see Figure 7c) in a region of alternating horizontal divergence ~~. During this time the trajectories cross back and forth over the dynamic tropopause~~(not shown explicitly).

~~The motion back and forth across the chosen PV value for~~ The analysis of the PV along the potential TST trajectories shows that these trajectories rather oscillate around the dynamic tropopause ~~becomes also evident from the PV along the trajectories (~~than cross the tropopause as coherent ensemble once and then reside in the lower stratosphere. This is somewhat evident in Figure 8a where only those trajectories are shown which at the physical start time of the trajectories have PV values initially smaller and at the last physical time step PV values larger than the respective dynamic tropopause PV value (here 2 pvu). The trajectories show no straight traverse from the troposphere into the stratosphere. However, several points shall be noted for the time close to the measurement briefly before 15 UTC. The static stability shows a maximum which is not evident in PV but accompanied by a strong decrease in relative vorticity towards anti-cyclonic flow (Figure 8b,e). The maximum in static stability follows a period where the trajectories encounter alternating vertical wind which is a sign of flow through small scale waves. At the end of this time period signs of turbulent motions increase. Initially, the turbulence index increases due to vertical wind shear as well as stretching and shearing deformation (Ellrod et al., 1992). Later low values of the Richardson number emerge which are indicative for KHI. The appearance of turbulence is further associated with a slight increase in potential temperature which is on the order of 1-2 K, thus the process can be regarded as quasi-isentropic.

The major difference between the three time periods between 14:20-14:54 UTC is the number of occurrence of these characteristic mixing trajectories, relative to the dynamic tropopause. During the first part between 14:20 - 14:36 UTC, we find only about 1.7 % out of ~~69048~~ 69,048 trajectories crossing the tropopause and have low Richardson numbers. This number increases to 23.9 % out of ~~51768~~ 51,768 in the second part and to 21.9 % out of ~~25920~~ 25,920 in the last part from 14:48 - 14:54 UTC. Notably, this result does not depend on the choice of our PV value for the dynamic tropopause. This indicates

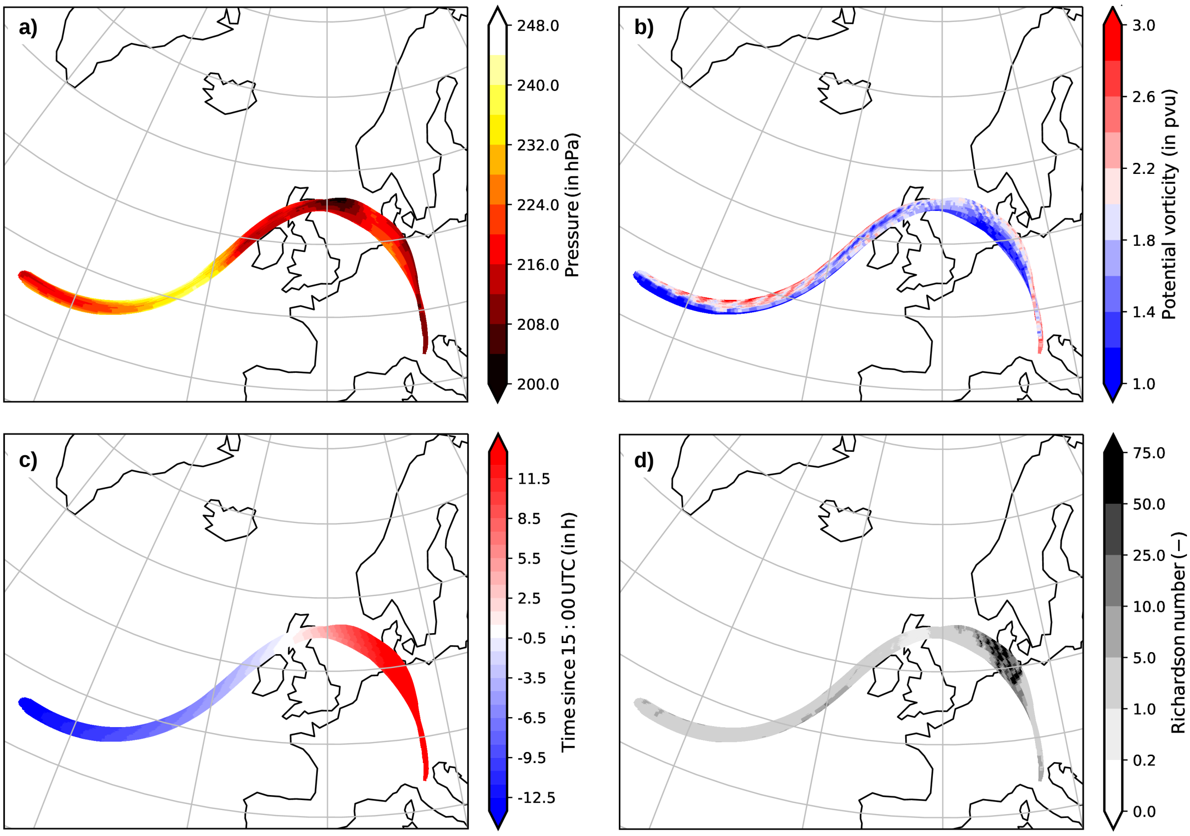

Figure 7. Trajectories crossing the 2 pvu isosurface and encountering a dynamic instability which cross the flight track between 14:36 – 14:48 UTC while HALO was flying on FL380. Trajectories start on 28.09.2017 01:00 UTC and end on 29.09.2017 11:00 UTC. The four panels show the following quantities along the trajectories: a) pressure (in hPa), b) potential vorticity (in pvu), c) time since 15:00 UTC (in h), and d) Richardson number. In total each panel shows ~~12375~~ 12,375 individual trajectories.

that a rather thick layer around the tropopause up to 3.5 pvu is affected by this mixing process, in particular in the between 14:36 - 14:48 UTC according to the trajectory analysis. Moreover, there is also a tendency of air masses from above to be mixed downward. For this we select trajectories which initially have a PV value above and finally below the desired dynamic tropopause value. While being most evident in the second and third part, such trajectories are in general much less common than those with an increasing PV value over the considered time period. In line with this is that the stratospheric influence on the measured air masses substantially decreases from the first to the third time period. While about two third of the trajectories originate in regions above 5 pvu in the first part, only about a quarter does in the second part and less than 0.5 $\%$ in the third part.

Consequently, the trajectory analysis shows that different air masses of tropospheric and stratospheric origin come together in the second and third part of the considered time period. This is in line with the measured trace gas concentrations of N_2O

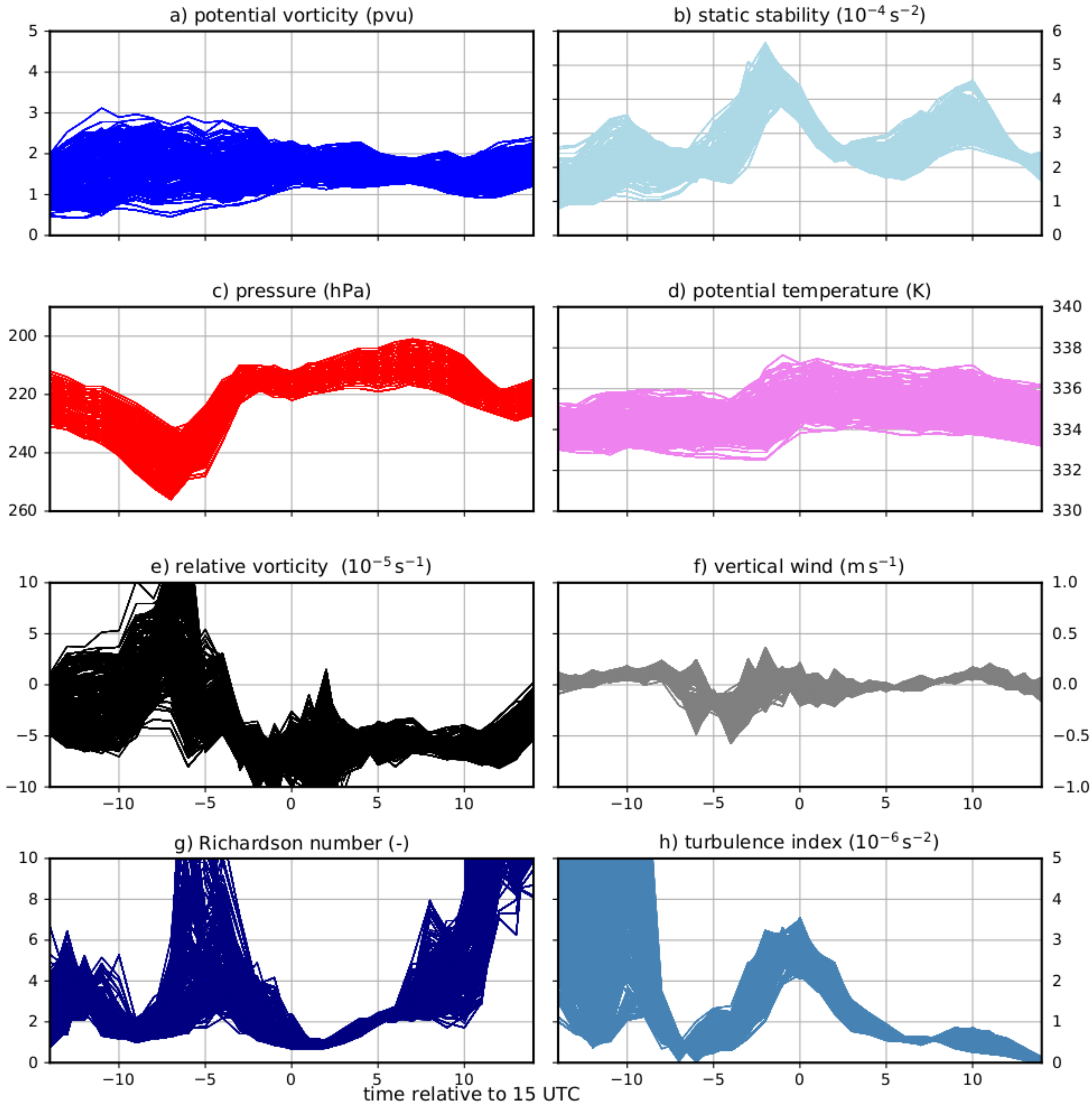

Figure 8. Time series of dynamic and thermodynamic quantities of mixing trajectories crossing the dynamic tropopause and experiencing a KHI. The time axis is relative to 28.09.2017 15 UTC. The eight panels show the following variables along the trajectories: a) potential vorticity (in pvu), b) static stability (in $10^{-4}\,\mathrm{s}^{-2}$), c) pressure (in hPa), d) potential temperature (in K), e) relative vorticity (in $10^{-5}\,\mathrm{s}^{-1}$), f) vertical wind (in ms^{-1}), g) Richardson number, and h) turbulence index after Ellrod et al. (1992) (in $10^{-6}\,\mathrm{s}^{-1}$).

and CO. However, based on the trajectory analysis it is difficult to ~~analyze~~ estimate whether STE and in particular TST ~~in a classical meaning occurs that an air parcel crosses~~ occurs in a way that air parcels cross the dynamic tropopause only once from the troposphere into the stratosphere and stay there afterwards. We also performed longer trajectory calculations which, however, ~~did not provide any further clear answer on whether STE in a classical meaning occurred or not. One reason could be~~ also provide no further evidence of TST trajectories which then reside in the stratosphere over a longer time period. We rather find trajectories which, based on PV, alternate back and forth between troposphere and stratosphere and which encounter low Richardson numbers along their paths. One potential reason why no TST trajectories are found which stay in the stratosphere is that the model fails to correctly resolve the process~~with the consequence that a clear STE can not be diagnosed from the trajectory calculations.~~. In contrast, assuming that the model performed well, it could simply mean that in this specific case the mixing occurred only across the tropopause with no substantial STE taking place. Independently on which is the case, this process changes the gradients of the trace gases in this region which in turn is of importance for radiative transfer calculations (e.g., Riese et al., 2012).

4 Mechanisms for mixing in ridges of baroclinic waves

After the analysis of airborne measurements, a first questions arises how generic such a mixing process may be in ridges of baroclinic waves. We can answer this question at least partly when searching for this process in idealized baroclinic life cycle experiments which are generic counterparts of atmospheric baroclinic waves. If the process is evident in the experiments, it might occur frequently in the real atmosphere and thus be of significance. Furthermore, the idealized experiments allow us to further analyze the physical processes which lead to mixing and potentially to STE. For this we use model results based on the idealized simulations already used in Kunkel et al. (2016). The simulations include non-conservative processes (in terms of PV) such as large scale and convective cloud microphysics, radiative effects from trace species and clouds, as well as vertical turbulence. These simulations were labeled with BRTC (BRTC = Bulk microphysics, Radiation, Turbulence, and Convection) in Kunkel et al. (2016). We further conducted simulations for life cycles 1 and 2 (Thorncroft et al., 1993), however, we focus our discussion here on results for life cycle 1. We extended the BRTC simulations by including tracers to mark the air which was initially in the stratosphere or troposphere as well as to trace the initial PV distribution. Furthermore, we calculated kinematic trajectories to analyze STE.

We first show that STE occurs in the model simulation. For this we calculated backward trajectories starting every six hours between 24 and 192 hours of model integration. The start points of these trajectories were distributed around the dynamic tropopause, i.e., the 2 pvu isosurface. They were initialized at each grid point in the horizontal and between 1.5 km below and 1.5 km above the local dynamic tropopause in the vertical. Each time more than ~~240.000~~ 240,000 trajectories are then traced back for six hours and consequently filtered based on whether they cross the tropopause. Furthermore, we searched for those STE trajectories which change their potential vorticity within the six hours by a given PV value to circumvent a residence time

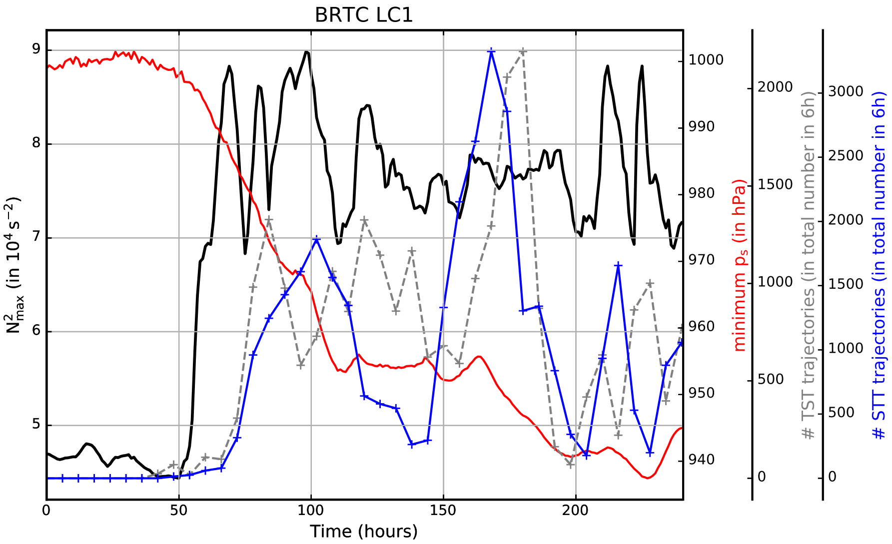

Figure 9. Temporal evolution of maximum static stability (black, in $10^{-4}\,s^{-2}$), minimum surface pressure (red, in hPa) as well as the number of TST and STT trajectories per six hour interval over the course of the idealized baroclinic life cycle experiment BRTC LC1. The maximum static stability N^2_{max} is derived by first averaging the static stability in the vertical between the altitudes of the local lapse rate tropopause and one kilometer above. The maximum value is then determined from the resulting two dimensional field over the horizontal model domain.

criterion suggested by Wernli and Bourqui (2002). For instance, we assume that trajectories which have an initial potential vorticity smaller than 1.5 pvu and a final one of larger 2.5 pvu have a larger ~~propability~~ probability to stay in the stratosphere than if the only criterion is to cross the 2 pvu isosurface.

The number of TST and STT trajectories based on these six hours long back trajectories reveal that STE starts to occur slightly after the time of the first enhancement of N^2 during the growing stage of the surface cyclone (Figure 9). Kunkel et al. (2016) attributed the increase of lower stratospheric static stability to updrafts in the troposphere. This can be regarded as the first time step when the tropopause is affected significantly by the tropospheric dynamics related to the baroclinic wave. Note that the initial state of the baroclinic life cycle experiments is designed such that the tropospheric background value is $N^2 = 1 \times 10^{-4}\,s^{-2}$ and that the stratospheric value is $N^2 = 4 \times 10^{-4}\,s^{-2}$. Peak values for STE are evident after 160 h of model integration, in the final stage of the life cycle (Reutter et al., 2015). ~~Thus, there is almost a temporal coincidence between the start of the enhancement of static stability and the first occurrence of STE.~~

We also find a spatial coincidence in the horizontal plane between the enhancement of N^2 above the thermal tropopause and TST across the dynamic tropopause by analyzing passive tracers in our idealized simulations (Figure 10). The tropospheric tracer, initialized with a constant non-zero mixing ratio in the troposphere and zero in the stratosphere, shows enhanced values at the first model layer in the stratosphere, exactly in the region where static stability is also enhanced. We define the first

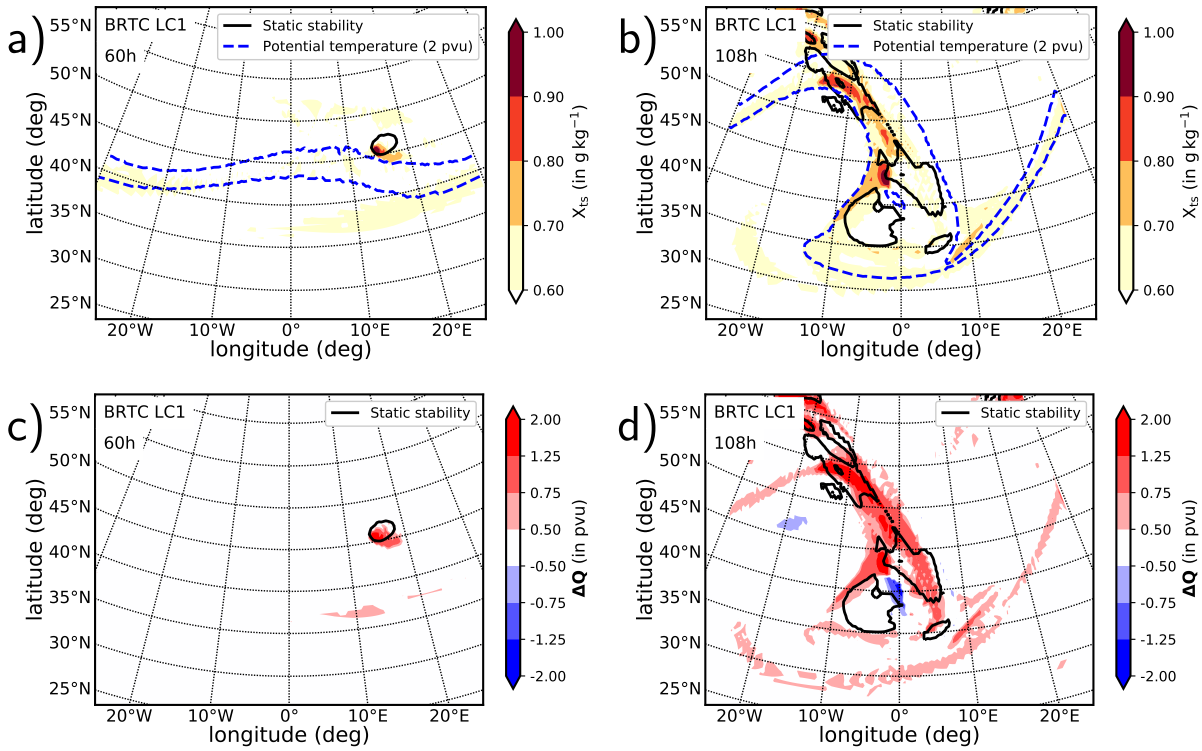

Figure 10. The tropospheric tracer X_{ts} on first full stratospheric level, i.e., the first full level with PV values larger 2 pvu for a) 60 h and b) 108 h after model start. Diabatic change of PV, $\Delta Q = Q - Q_{0,\mathrm{adv}}$, at the level of the dynamic tropopause with $Q_{0,\mathrm{adv}}$ being the advected initial PV and Q being the full PV for c) 60 h and d) 108 h after model start. The black isoline shows static stability, $N^2 = 5.5 \times 10^{-4}\,\mathrm{s}^{-2}$. The blue dashed lines show isolines of potential temperature for 315 K and 325 K.

model level in the stratosphere as the first full model level above the dynamic tropopause. This region also marks the region where the tropospheric tracer enters the stratosphere. This is first evident after about 60 h (Figure 10a), but also at later time steps (Figure 10b). We further can confirm these findings based on our diabatic PV tracer. This tracer carries the information about the difference between the current and the initial value of PV in each grid box (Kunkel et al., 2014). Evaluating this difference on the dynamic tropopause allows us to diagnose whether an airmass at the dynamic tropopause gained or lost PV, thus whether this air mass initially resided in the troposphere or in the stratosphere. Positive values of this difference indicate a gain of PV, i.e., TST, and negative values a loss of PV, i.e., STT, of the respective air mass at the dynamic tropopause since model start (Figure 10c,d). In contrast to TST and although a temporal coincidence is also evident for N^2 enhancement and occurrence of STT, no spatial co-occurrence is evident for STT in regions of enhanced N^2 (Figures 10c,d; and also based on the analysis of the stratospheric tracer which is not shown explicitly here). Thus, from the distribution of these passive tracers, we can conclude that there is also a spatial coincidence between TST and enhancement of static stability.

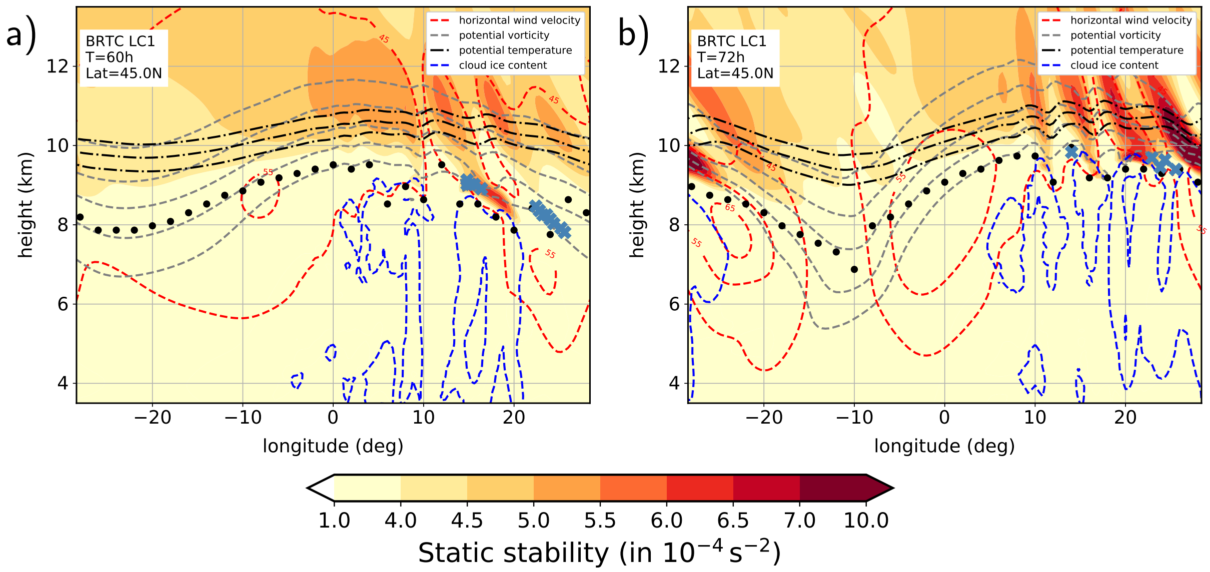

Figure 11. Zonal cross sections along the center of the model domain at 45 °N show static stability (contour filled), potential temperature (330 K, 335 K, 340 K, black lines), cloud ice water content ($10 \times 10^{-6}\,\mathrm{kg\,kg^{-1}}$, blue lines), potential vorticity (2-6 pvu, ~~grey~~ gray lines), as well as the altitude of the thermal tropopause (black dots). Red lines show isolines of the horizontal wind speed (45-65 $\mathrm{ms^{-1}}$) and blue crosses show points of trajectories at the respective longitude which cross the tropopause from the troposphere to the stratosphere over the course of the last six hours for a) 60 h and b) 72 h after model start.

Furthermore, the exchange occurs in the ridge of the baroclinic wave, just above a region of ice cloud occurrence (Figure 11). This region is also strongly affected by a small scale wave pattern related to a propagating inertia gravity wave which is evident in the isolines of potential temperature and PV. This wave is one source of the enhanced values of static stability. The other source is radiative cooling below and at the tropopause related to ice clouds in the upper troposphere. The first time TST occurs in this region is after about 60 h, while it is evidently more frequent during later stages of the life cycle. We thus ~~found~~ find a pathway from the troposphere into the stratosphere in the ridge of baroclinic waves in our idealized simulations. The situation is as initially expected from the results of Kunkel et al. (2016) and resembles the situation of the mixing and potential TST in the ridge during WISE RF07.

Before we end our discussion by studying the processes leading to mixing, we want to highlight the fact that in our idealized simulations two type of TST trajectories are apparent (Figure 12). One set of TST trajectories exhibits low values of static stability, low potential temperatures, positive relative vorticity, and moderate turbulent kinetic energy (TKE). In contrast, the other set of TST trajectories shows large values of static stability, higher potential temperatures, negative relative vorticity, and larger values of TKE. Thus, while the first set of trajectories crosses the tropopause at the cyclonic side of the jet at rather low altitudes, the other set of trajectories crosses the tropopause at the anti-cyclonic side of the jet at rather high altitudes. Such

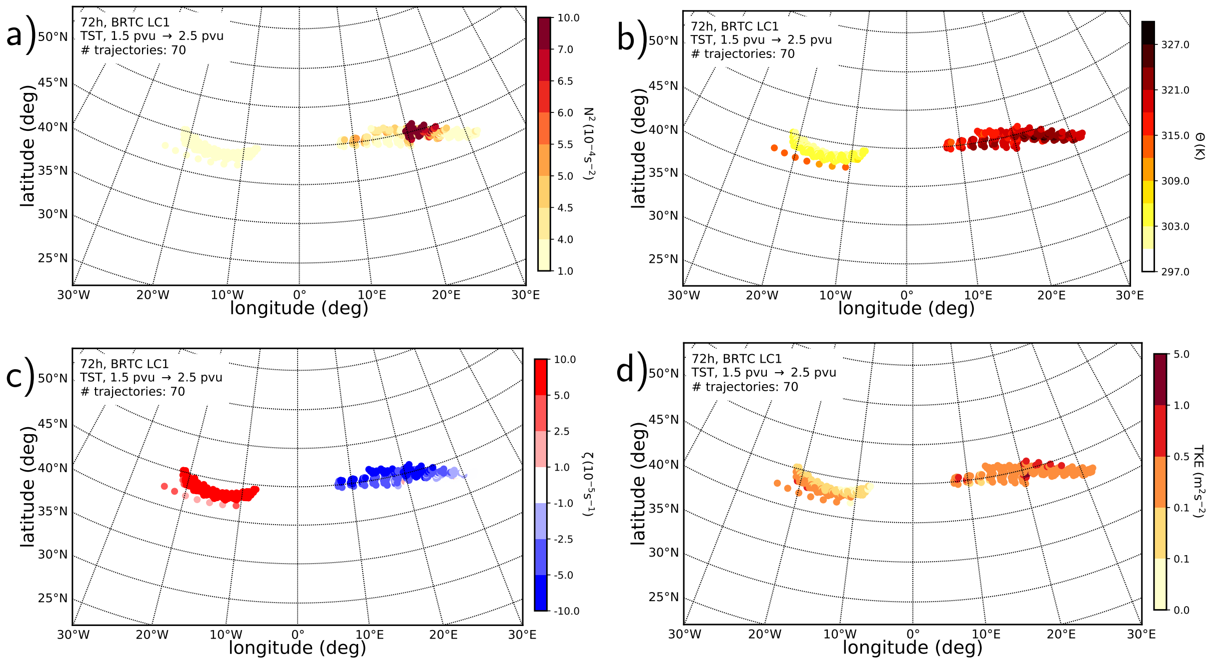

Figure 12. Trajectories starting 66 h and ending 72 h after model start which increase their PV from values smaller than 1.5 pvu to values larger 2.5 pvu within the six hour interval. Panels show a) static stability (in $10^{-4}\,\mathrm{s}^{-2}$), b) potential temperature (in K), c) relative vorticity (in $10^{-5}\,\mathrm{s}^{-1}$), and turbulent kinetic energy (in $\mathrm{m}^2\,\mathrm{s}^{-2}$) along the trajectories for each hour.

trajectories are found over a large part of the life cycle, also in the case when we apply different criteria for a change of PV, e.g., from 1.5 pvu to 3.0 pvu. A common feature of the two sets of trajectories is that in both cases the potential temperature values hardly change in the six hours; thus, the TST occurs quasi-isentropically. We also note that the trajectories crossing the tropopause in the ridge of the wave experience large values of static stability, thus ~~passoin through the tropopause inversion layer.~~ passing through the TIL. Thus, what initially might seem counter-intuitive, i.e., the exchange in the vicinity of large values of static stability inhibiting vertical motions, is nevertheless possible in the ridge of the baroclinic waves.

The last point that we want to address are the processes causing the mixing and exchange across the tropopause in the ridge of the baroclinic wave. The occurrence of turbulence becomes apparent by low values of the Gradient Richardson number and enhanced values of TKE (Figure 13). The Richardson number is the ratio between static stability and vertical shear of the horizontal wind. Since static stability shows rather large values above the tropopause, the source of low Richardson numbers results from large vertical shear of the horizontal wind (Figure 14a). The shear is largest in the ridge where a gravity wave is evident at the edges of the jet-stream. The shear also contributes to enhanced values of TKE and might thus explain its enhancement. However, TKE further depends on the vertical gradient of the total moisture which can consequently lead to a buoyant heat flux (Doms, 2011). This buoyant heat flux shows positive and negative values at the tropopause, most probably related

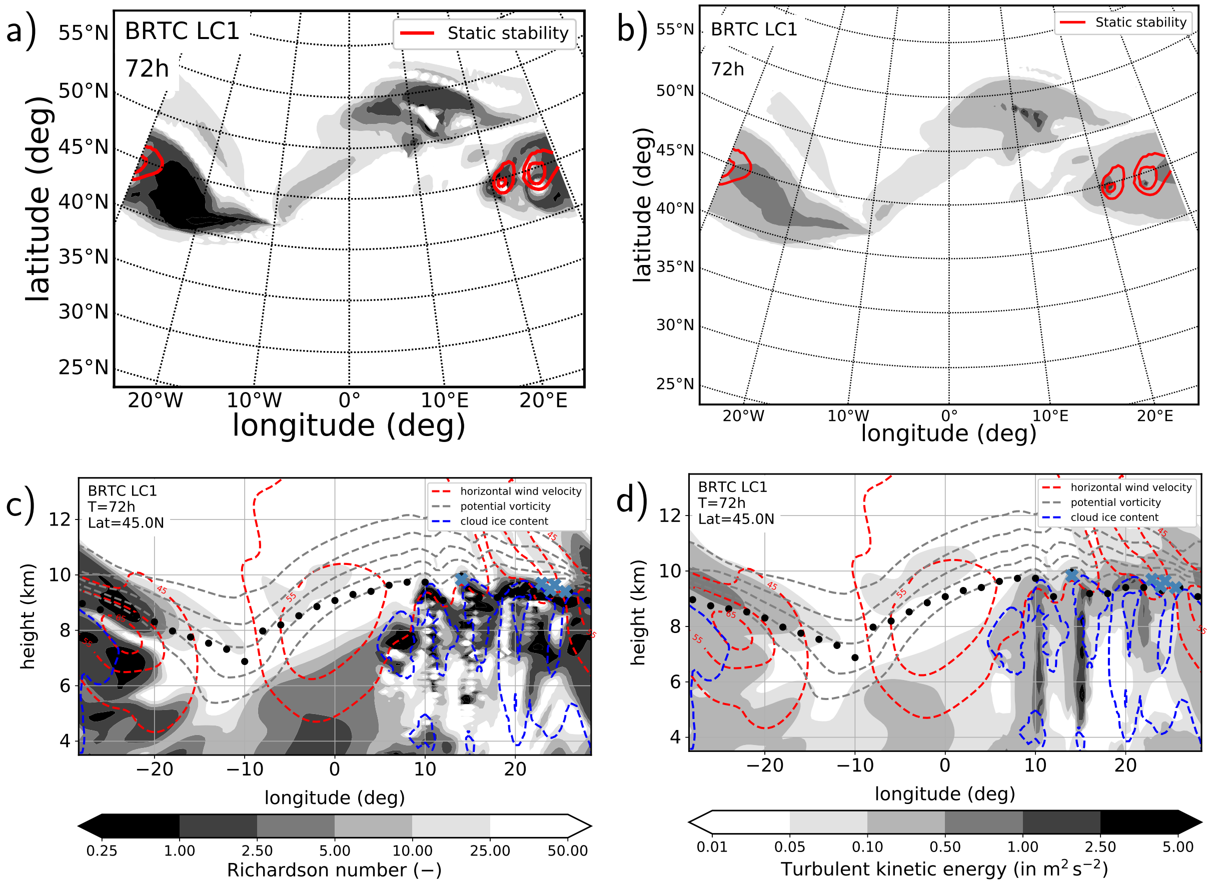

Figure 13. Left panels a) and c) show gradient Richardson number, Ri, right panels b) and d) TKE after 72 h of model integration. Upper panels show a horizontal ~~cross-sectionw~~ cross-section at the dynamic tropopause along with isolines of static stability with values of $N^2 = 5.5 \times 10^{-4}\,\mathrm{s}^{-2}$ and $N^2 = 7.0 \times 10^{-4}\,\mathrm{s}^{-2}$, lower panels show zonal cross sections at 45°N in the center of the model domain, including isolines of various variables (see detailed description in Figure 11).

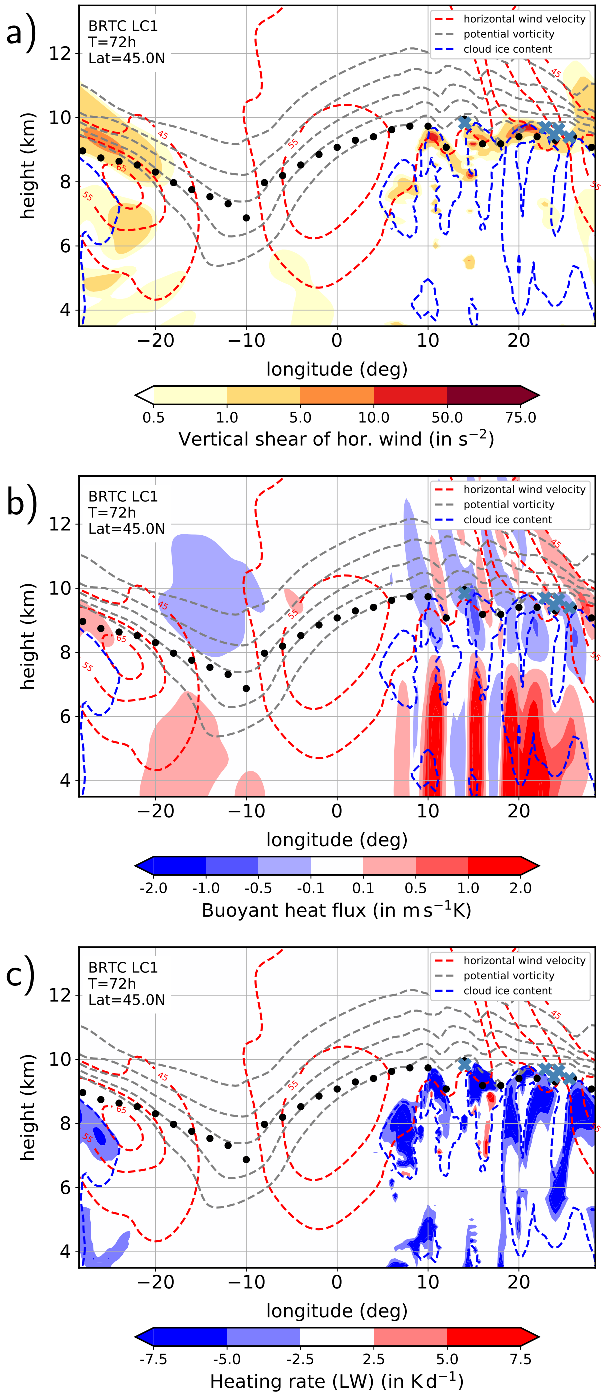

Figure 14. Zonal cross sections of a) vertical shear of horizontal wind S^2, b) buoyant heat flux $w'\Theta_v'$, and c) long wave heating rate $D\Theta_{LW}/Dt$ at 45 °N and after 72 h of model integration. For the description of isolines it is referred to Figure 11.

to the propagating and potentially dissipating gravity wave (Figure 14b). In particular, in the region of the TST trajectories negative values are dominant which could indicate upward motions in an otherwise stable environment. The stability is further increased by a radiative feedback of the ice clouds (Figure 14c). ~~Coolling~~ Cooling is evident at the top of the clouds which in turn enhances the static stability above the tropopause in the region of the mixing (e.g., Fusina and Spichtinger, 2010; Kunkel et al., 2016). Thus, we identified the processes which allow for mixing induced by shear in a region which is stably stratified.

5 Summary and conclusions

A recent study by Kunkel et al. (2016) showed the concurrent occurrence of enhanced static stability in the lower stratosphere and increased turbulent motions across the extratropical tropopause in the ridge of idealized baroclinic life cycles. Here, we present evidence that such a situation corresponds with mixing of trace gases at the level of or slightly above the tropopause and eventually with transport of tropospheric air into the stratosphere. To the authors' knowledge this process has gained only little attention so far, in particular in terms of the formation of the extratropical transition layer. We derive our conclusions from airborne measurements along with high resolution ECMWF model data to identify the occurrence of mixing and potential TST in the ridge of a baroclinic wave. We further extended experiments of idealized baroclinic life cycles from Kunkel et al. (2016) to elucidate the driving mechanisms and to ~~assess~~ obtain a more general picture of the mixing process.

During WISE RF07 signs of turbulent mixing are evident between 335-340 K potential temperature in the lowermost stratosphere just above the tropopause. The region of interest was situated above an extended cloud deck associated with a warm conveyor belt outflow and was substantially affected by small scale waves in the lowermost stratosphere. Vertical profiles of tracers with a sufficient long life time in the UTLS such as CO and N_2O and their correlations are used to identify quasi-isentropic mixing between air masses of different origin. In particular, the N_2O tracer mixing ratios suggest that tropospheric and stratospheric air masses mix in this region. Power spectral densities of potential temperature support the analysis suggesting that rather meso- than synoptic scale processes affect the power spectrum in the region of mixing.

Furthermore, ECMWF forecast data with the highest available resolution are used to obtain a broader view on the synoptic situation. Although the model performs well in representing the overall situation, some deviations have been found between model and measurements. In particular, these deviations occur at small scales which seem to be substantial in the representation of the mixing process. Nevertheless, trajectory calculations based on the model data show that mixing occurs around the tropopause and affects the lower part of the extratropical transition layer. The mixing occurs in regions of enhanced lower stratospheric static stability, ~~relative~~ relatively high potential temperature, anti-cyclonic flow, and during a time when the flow is affected by vertical shear, deformation, and moderate alternating vertical motions.

Moreover, numerical experiments of idealized baroclinic life cycles support the observational findings. In the model simulations it is evident that mixing occurs in the ridge of baroclinic waves, just above the top of ice clouds. Using special tracers and kinematic trajectories, we showed that even TST occurs in regions of enhanced static stability, thus in the region of the ~~tropopause inversion layer.~~ TIL. To a large degree the mixing is the result of a Kelvin-Helmholtz instability which has its source in enhanced vertical shear as has recently been demonstrated by ~~Kaluza et al. (2018)~~Kaluza et al. (2019). This shear is strongly related to inertia-gravity wave dynamics at the upper edge of the jet-stream. Moreover, buoyant heat fluxes caused by the upper-tropospheric clouds may also enhance the turbulence across the tropopause.

The overall relevance of this process needs yet to be analyzed. This is beyond of the current study. However, on the one hand this process occurs on small scales, and is related to cirrus clouds at the tropopause and a strong wind shear which in turn seems to be related to small scale waves in the lower stratosphere. Thus, the impact on the trace gases in the upper troposphere and lower stratosphere might be not particularly large due to the limited geographical extent of the combinations of these processes. On the other hand all this occurs within baroclinic life cycles which ~~in turn~~ are relatively frequent features of the extratropical UTLS. Thus, there is potentially a non-negligible contribution of this mixing process on the composition of the extratropical transition layer. In particular, since this mixing occurs at relatively high potential temperatures, it can affect regions which have previously not been considered to be strongly affected by STE in baroclinic waves. Previous studies showed that the main exchange in the extratropics occurs at lower potential temperature levels at the lower edge of the jet-stream.

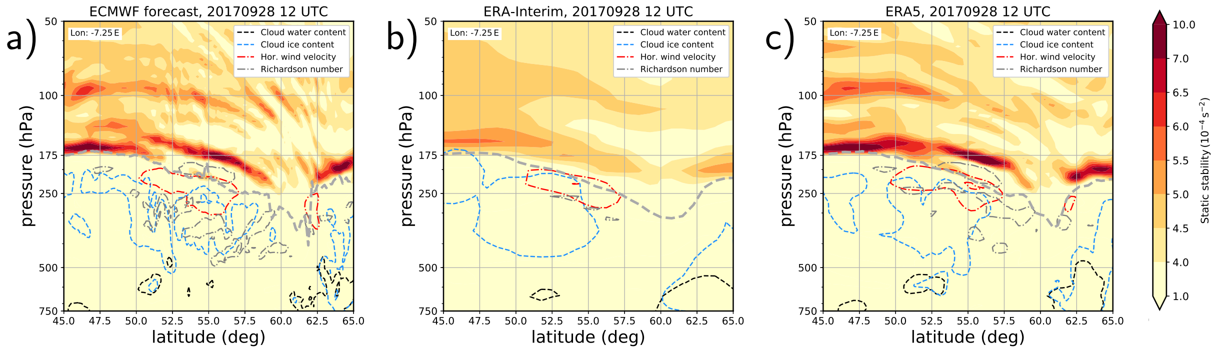

Figure 15. Zonal cross sections along $-7.25\,°$E at 28.09.2017 12 UTC show static stability (color shaded), the altitude of the 2 pvu isosurface (light ~~grey~~gray), cloud water content (black), cloud ice content (blue), horizontal wind speed (red), and Richardson number (dark ~~grey~~gray). The three panels show a) the ECMWF forecast (with 0.07° horizontal grid spacing and $\sim$ 300 m vertical grid point spacing in the UTLS), b) the ERA Interim reanalysis (with 0.75° horizontal grid spacing and $\sim$ 1000 m vertical grid spacing), and c) the ERA5 reanalysis (with 0.25° horizontal grid spacing and $\sim$ 300 m vertical grid spacing).

One reason why the process described in this study has not gained much attention is that numerical weather prediction models and in particular reanalysis products as well as climate models do not resolve the UTLS sufficiently, thus potentially miss or misrepresent the relevant processes. However, especially reanalysis data sets build the basis for almost all recent climatological studies of STE (e.g., Škerlak et al., 2014; Boothe and Homeyer, 2017). Figure 15 shows the same cross section for different ECMWF products. While the forecast shows many fine scale features, e.g., in the cloud structure and the location of the tropopause, these features are almost entirely missing in ERA Interim. This is to a large degree caused by the poorer vertical resolution of ERA Interim which is similar to the resolution in current climate models. In contrast, the new ERA5 reanalysis data which uses the same vertical grid spacing as the current forecast model shows more similarity to the forecast and might thus allow for a better representation of STE in the extratropics than ERA Interim. However, potentially even the forecast data still has problems to fully capture all features correctly, because the vertical grid spacing of that data is still relatively coarse compared to our idealized simulations with a vertical grid spacing of 110 m and a horizontal grid spacing of 0.4° which captured the TST relatively well. Thus, an increase of vertical model resolution seems to be necessary to further address this process and its potential consequences also on the larger scale.

Code and data availability. ECMWF (forecast, ERA Interim and ERA5) data has been retrieved from the MARS server. The airborne measurement data from the WISE campaign are available through the HALO data base (https://halo-db.pa.op.dlr.de/). The code of the COSMO model is available on request from the COSMO consortium (http://www.cosmo-model.org/). LAGRANTO is available from http://iacweb.ethz.ch/staff//sprenger/lagranto/. Output from the idealized COSMO simulations is available upon request (dkunkel@uni-mainz.de).

Appendix A: Idealized model setup

The model setup described here has also been used in Kunkel et al. (2016). Additionally, more information can be found in Kunkel et al. (2014) where only a version without parameterized physics has been used.

We use the non-hydrostatic regional model COSMO in an idealized, spherical, midlatitude channel configuration (COSMO: COnsortium for Small-scale MOdelling Steppeler et al., 2003). The dynamical core of the model solves the hydro-thermodynamical equations. A fourth-order horizontal hyper-diffusion has to be applied to guarantee numerical stability. Time integration is performed with a third-order Runge–Kutta scheme. Passive tracer advection is done with a fourth-order Bott scheme with Strang splitting.

Physical parameterizations have been included in our simulations for turbulence, radiation, large-scale, and convective clouds. These processes are included in the acronym of the simulation BRTC (B: bulk microphysics, R: radiation, T: turbulence, and C: convection).

Turbulence is calculated for the three-dimensional wind, the liquid water potential temperature, and the total water. Budget equations for the second-order moments are reduced under application of a closure of level 2.5 (in the notation of Mellor and Yamada (1982)), i.e., local equilibrium is assumed for all moments except for turbulent kinetic energy (TKE), for which advection and turbulent transport is retained. Only vertical turbulent fluxes are parameterized under consideration of the Boussinesq approximation. Moreover, the TKE budget equation depends significantly on the vertical shear of the horizontal wind components and the vertical change in liquid water potential temperature and total water.

Radiation is parameterized by the δ-2 stream approximation, i.e., separate treatment of solar and terrestrial wavelengths. In total, eight spectral bands are considered, five in the solar range and three infrared bands. Absorbing and scattering gases are water vapor with a variable content as well as CO_2, O_3, CH_4, N_2O, and O_2 with fixed amounts. Aerosols have been totally neglected whereas a cloud radiative feedback can be calculated in all spectral bands.

Large scale cloud microphysics follow a bulk approach using a single moment scheme with five types of water categories being treated prognostically: specific humidity, cloud water and ice, as well as rain and snow. These five water types can interact within various processes such as cloud condensation and evaporation, depositional growth and sublimation of snow, evaporation of snow and rain, melting of snow and cloud ice, homogeneous and heterogeneous nucleation of cloud ice, autoconversion, collection, and freezing. The scheme of Tiedtke (1989) is used to parameterize subgrid-scale convective clouds and their effects on the large-scale environment. This approach uses moisture convergence in the boundary layer to estimate the cloud base mass flux. The convection scheme then affects the large-scale budgets of the environmental dry static energy, the specific humidity, and the potential energy.

The baroclinic waves have a wavenumber six. The model domain spans over 60 degrees longitude and 70 degrees latitude with a grid spacing of 0.4 degrees in the horizontal and 110 m in the vertical from the surface up to 25 km. In the uppermost 7 km of the model domain, Rayleigh damping is applied to avoid reflection of upward propagating signals; the surface of the model domain is flat. In the meridional direction the boundary conditions are relaxed towards the initial values to avoid reflection of outgoing signals, while periodic boundary conditions are specified in the zonal direction.

The initial conditions consist of a background state and of a superimposed anomaly of potential vorticity. The background state for temperature, pressure, and horizontal wind is by construction baroclinically unstable. The anomaly of potential vorticity is introduced at the altitude of the tropopause. This anomaly can be inverted to obtain perturbations fields for p, T, u, v. Slight changes in these initial conditions allow us to study various types of baroclinic waves. In our study we focus on life cycles of type 1 (LC1, Thorncroft et al., 1993). If an additional barotropic shear is considered during construction of the background state life cycles of type 2 (LC2) can be created. More information on the initial conditions and the model setup in general can be found in Kunkel et al. (2014, 2016, and references therein).

Author contributions. DK and PH designed the study. MR, MK, PH, DK organized the WISE campaign and were part of the scientfic flight planning team. DK, PH, BK analyzed the in situ data from WISE and JU provided GLORIA data. DK and TK analyzed ECMWF model

data. DK ran the idealized simulations and analyzed the data with input from PH. DK wrote the paper with input from PH and TK; all authors contributed to the manuscript.

Competing interests. No competing interests.

Acknowledgements. Special thanks to the entire WISE team for the successful campaign. Logistics were handled by DLR-FX; many thanks for the great support and organization before, during, and after the campaign. Also a special thanks to the pilots for the realization of the specific flight patterns. More information about the WISE campaign can be found at https://www.wise2017.de/. We further thank all members of the GLORIA instrument team for their large efforts in developing the first airborne IR limb imager. The GLORIA hardware was mainly funded by the Helmholtz Association of German Research Centres through several large investment funds. The authors also thank H. Wernli and M. Sprenger for the possibility to use LAGRANTO for this study. The authors are grateful to ECMWF for providing operational analysis and forecast as well as reanalysis data through the MARS server. The Authors acknowledge funding from the German Science Foundation, as this study was carried out as part of the preparation phase for the WISE campaign under funding from the HALO SPP 1294 (DFG grant no. KU 3524/1-1, HO 4225/7-1 as well as HO 4225/8-1). Parts of this research were conducted using the supercomputer Mogon and advisory services offered by Johannes Gutenberg University Mainz (hpc.uni-mainz.de), which is a member of the AHRP (Alliance for High Performance Computing in Rhineland Palatinate, www.ahrp.info) and the Gauss Alliance e.V. The authors gratefully acknowledge the computing time granted on the supercomputer Mogon at Johannes Gutenberg University Mainz (hpc.uni-mainz.de).

References

Appenzeller, C., Davies, H. C., and Norton, W. A.: Fragmentation of stratospheric intrusions, Journal of Geophysical Research Atmospheres, 101, 1435–1456, https://doi.org/10.1029/95JD02674, 1996.

Birner, T. and Bönisch, H.: Residual circulation trajectories and transit times into the extratropical lowermost stratosphere, Atmospheric Chemistry and Physics, 11, 817–827, https://doi.org/10.5194/acp-11-817-2011, 2011.

Birner, T., Dörnbrack, A., and Schumann, U.: How sharp is the tropopause at midlatitudes?, Geophysical Research Letters, 29, 1–4, https://doi.org/10.1029/2002GL015142, 2002.

Boothe, A. C. and Homeyer, C. R.: Global large-scale stratosphere-troposphere exchange in modern reanalyses, Atmospheric Chemistry and Physics, 17, 5537–5559, https://doi.org/10.5194/acp-17-5537-2017, 2017.

Bush, A. B. G. and Peltier, W. R.: Tropopause Folds and Synoptic-Scale Baroclinic Wave Life Cycles, Journal of the Atmospheric Sciences, 51, 1581–1604, https://doi.org/10.1175/1520-0469(1994)051<1581:TFASSB>2.0.CO;2, 1994.

Butchart, N.: The Brewer-Dobson circulation, https://doi.org/10.1002/2013RG000448, 2014.

Chagnon, J. M., Gray, S. L., and Methven, J.: Diabatic processes modifying potential vorticity in a North Atlantic cyclone, Quarterly Journal of the Royal Meteorological Society, 139, 1270–1282, https://doi.org/10.1002/qj.2037, 2013.

Chen, P.: Isentropic cross-tropopause mass exchange in the extratropics, Journal of Geophysical Research, 100, 16 661–16 673, http://www.agu.org/journals/jd/v100/iD08/95JD01264/, 1995.

Danielsen, E. F.: Stratospheric-Tropospheric Exchange Based on Radioactivity, Ozone and Potential Vorticity, Journal of the Atmospheric Sciences, 25, 502–518, https://doi.org/10.1175/1520-0469(1968)025<0502:STEBOR>2.0.CO;2, 1968.

Danielsen, E. F., Hipskind, R. S., Starr, W. L., Vedder, J. F., Gaines, S. E., Kley, D., and Kelly, K. K.: Irreversible transport in the stratosphere by internal waves of short vertical wavelength, Journal of Geophysical Research, 96, 17 433, https://doi.org/10.1029/91JD01362, 1991.

Dethof, A., O'Neill, A., and Slingo, J.: Quantification of the isentropic mass transport across the dynamical tropopause, Journal of Geophysical Research Atmospheres, 105, 12 279–12 293, https://doi.org/10.1029/2000JD900127, 2000.

Doms, G.: A Description of the Nonhydrostatic Regional COSMO-Model, Part I: Dynamics and Numerics, Tech. rep., Deutscher Wetterdienst, Offenbach, Germany, 2011.

Ellrod, G. P., Knapp, D. I., Ellrod, G. P., and Knapp, D. I.: An Objective Clear-Air Turbulence Forecasting Technique: Verification and Operational Use, Weather and Forecasting, 7, 150–165, https://doi.org/10.1175/1520-0434(1992)007<0150:AOCATF>2.0.CO;2, 1992.

Fischer, H., Wienhold, F. G., Hoor, P., Bujok, O., Schiller, C., Siegmund, P., Ambaum, M., Scheeren, H. A., and Lelieveld, J.: Tracer correlations in the northern high latitude lowermost stratosphere: Influence of cross-tropopause mass exchange, Geophysical Research Letters, 27, 97–100, https://doi.org/10.1029/1999GL010879, 2000.

Forster, C. and Wirth, V.: Radiative decay of idealized stratospheric filaments in the troposphere, Journal of Geophysical Research: Atmospheres, 105, 10 169–10 184, https://doi.org/10.1029/2000JD900052, 2000.

Friedl-Vallon, F., Gulde, T., Hase, F., Kleinert, A., Kulessa, T., Maucher, G., Neubert, T., Olschewski, F., Piesch, C., Preusse, P., Rongen, H., Sartorius, C., Schneider, H., Tan, V., Bayer, N., Blank, J., Dapp, R., Ebersoldt, A., Fischer, H., Graf, F., Guggenmoser, T., Kaufmann, M., Kretschmer, E., Latzko, T., Nordmeyer, H., Oelhaf, H., Orphal, J., Riese, M., Schardt, G., Schillings, J., Sha, M. K., and Ungermann, J.: Instrument concept of the imaging Fourier transform spectrometer GLORIA, Atmospheric Measurement Techniques, 7, 3565–3577, https://doi.org/10.5194/amt-7-3565-2014, 2014.

Fusina, F. and Spichtinger, P.: Cirrus clouds triggered by radiation, a multiscale phenomenon, Atmospheric Chemistry and Physics, 10, 5179–5190, https://doi.org/10.5194/acp-10-5179-2010, 2010.

Gettelman, A., Hoor, P., Pan, L. L., Randel, W. J., Hegglin, M. I., and Birner, T.: The extratropical upper troposphere and lower stratosphere, Reviews of Geophysics, 49, RG3003, https://doi.org/10.1029/2011RG000355, 2011.

Gray, S. L.: Mechanisms of midlatitude cross-tropopause transport using a potential vorticity budget approach, Journal of Geophysical Research: Atmospheres, 111, https://doi.org/10.1029/2005JD006259, 2006.

Grise, K. M., Thompson, D. W. J., and Birner, T.: A Global Survey of Static Stability in the Stratosphere and Upper Troposphere, Journal of Climate, 23, 2275–2292, https://doi.org/10.1175/2009JCLI3369.1, 2010.

Hegglin, M. I., Boone, C. D., Manney, G. L., and Walker, K. a.: A global view of the extratropical tropopause transition layer from Atmospheric Chemistry Experiment Fourier Transform Spectrometer O 3 , H 2 O, and CO, Journal of Geophysical Research, 114, D00B11, https://doi.org/10.1029/2008JD009984, 2009.

Holton, J. R., Haynes, P. H., McIntyre, M. E., Douglass, A. R., Rood, R. B., and Pfister, L.: Stratosphere-troposphere exchange, Reviews of Geophysics, 33, 403, https://doi.org/10.1029/95RG02097, 1995.

Homeyer, C. R.: Numerical simulations of extratropical tropopause penetrating convection: Sensitivities to grid resolution, Journal of Geophysical Research, 120, 7174–7188, https://doi.org/10.1002/2015JD023356, 2015.

Homeyer, C. R., Pan, L. L., Dorsi, S. W., Avallone, L. M., Weinheimer, A. J., O'Brien, A. S., DiGangi, J. P., Zondlo, M. A., Ryerson, T. B., Diskin, G. S., and Campos, T. L.: Convective transport of water vapor into the lower stratosphere observed during double tropopause events, Journal of Geophysical Research: Atmospheres, p. 2014JD021485, https://doi.org/10.1002/2014JD021485, 2014.

Hoor, P., Fischer, H., Lange, L., Lelieveld, J., and Brunner, D.: Seasonal variations of a mixing layer in the lowermost stratosphere as identified by the CO-O 3 correlation from in situ measurements, Journal of Geophysical Research: Atmospheres, 107, ACL 1–1–ACL 1–11, https://doi.org/10.1029/2000JD000289, 2002.

Hoor, P., Gurk, C., Brunner, D., Hegglin, M. I., Wernli, H., and Fischer, H.: Seasonality and extent of extratropical TST derived from in-situ CO measurements during SPURT, Atmospheric Chemistry and Physics, 4, 1427–1442, https://doi.org/10.5194/acp-4-1427-2004, 2004.

Hoskins, B. J., McIntyre, M. E., and Robertson, A. W.: On the use and significance of isentropic potential vorticity maps, Quarterly Journal of the Royal Meteorological Society, 111, 877–946, https://doi.org/10.1002/qj.49711147002, 1985.

Jaeger, E. B. and Sprenger, M.: A Northern Hemispheric climatology of indices for clear air turbulence in the tropopause region derived from ERA40 reanalysis data, Journal of Geophysical Research, 112, D20 106, https://doi.org/10.1029/2006JD008189, 2007.

Joos, H. and Wernli, H.: Influence of microphysical processes on the potential vorticity development in a warm conveyor belt: a case-study with the limited-area model COSMO, Quarterly Journal of the Royal Meteorological Society, 138, 407–418, https://doi.org/10.1002/qj.934, 2012.

Kaluza, T., Kunkel, D., and Hoor, P.: Composite analysis of the tropopause inversion layer in extratropical baroclinic waves, Atmospheric Chemistry and Physics Discussions, pp. 1–22, https://doi.org/10.5194/acp-2018-1100, 2018.

Kaluza, T., Kunkel, D., and Hoor, P.: Composite analysis of the tropopause inversion layer in extratropical baroclinic waves, Atmospheric Chemistry and Physics, 19, 6621–6636, https://doi.org/10.5194/acp-19-6621-2019, 2019.

Kaufmann, M., Blank, J., Guggenmoser, T., Ungermann, J., Engel, A., Ern, M., Friedl-Vallon, F., Gerber, D., Grooß, J. U., Guenther, G., Höpfner, M., Kleinert, A., Kretschmer, E., Latzko, T., Maucher, G., Neubert, T., Nordmeyer, H., Oelhaf, H., Olschewski, F., Orphal, J., Preusse, P., Schlager, H., Schneider, H., Schuettemeyer, D., Stroh, F., Suminska-Ebersoldt, O., Vogel, B., M. Volk, C., Woiwode, W., and

Riese, M.: Retrieval of three-dimensional small-scale structures in upper-tropospheric/lower-stratospheric composition as measured by GLORIA, Atmospheric Measurement Techniques, 8, 81–95, https://doi.org/10.5194/amt-8-81-2015, 2015.

Konopka, P. and Pan, L. L.: On the mixing-driven formation of the Extratropical Transition Layer (ExTL), Journal of Geophysical Research, 117, D18 301, https://doi.org/10.1029/2012JD017876, 2012.

Krause, J., Hoor, P., Engel, A., Plöger, F., Grooß, J. U., Bönisch, H., Keber, T., Sinnhuber, B. M., Woiwode, W., and Oelhaf, H.: Mixing and ageing in the polar lower stratosphere in winter 2015-2016, Atmospheric Chemistry and Physics, 18, 6057–6073, https://doi.org/10.5194/acp-18-6057-2018, 2018.

Krautstrunk, M. and Giez, A.: The Transition From FALCON to HALO Era Airborne Atmospheric Research, pp. 609–624, Springer, Berlin, Heidelberg, https://doi.org/10.1007/978-3-642-30183-4_37, 2012.

Kunkel, D., Hoor, P., and Wirth, V.: Can inertia-gravity waves persistently alter the tropopause inversion layer?, Geophysical Research Letters, 41, n/a–n/a, https://doi.org/10.1002/2014GL061970, 2014.

Kunkel, D., Hoor, P., and Wirth, V.: The tropopause inversion layer in baroclinic life-cycle experiments: the role of diabatic processes, Atmospheric Chemistry and Physics, 16, 541–560, https://doi.org/10.5194/acp-16-541-2016, 2016.

Lamarque, J.-F. and Hess, P. G.: Cross-Tropopause Mass Exchange and Potential Vorticity Budget in a Simulated Tropopause Folding, Journal of the Atmospheric Sciences, 51, 2246–2269, https://doi.org/10.1175/1520-0469(1994)051<2246:CTMEAP>2.0.CO;2, 1994.

Lamarque, J.-F., Langford, A. O., and Proffitt, M. H.: Cross-tropopause mixing of ozone through gravity wave breaking: Observation and modeling, Journal of Geophysical Research: Atmospheres, 101, 22 969–22 976, https://doi.org/10.1029/96JD02442, 1996.

Langford, A. O., Proffitt, M. H., and Vanzandt, T. E.: Modulation of tropospheric ozone by a propagating gravity wave, Journal of Geophysical Research: Atmospheres, 101, 26 605–26 613, https://doi.org/0148-0227/96/96JD-0242, 1996.

Mellor, G. L. and Yamada, T.: Development of a turbulence closure model for geophysical fluid problems, Reviews of Geophysics, 20, 851, https://doi.org/10.1029/RG020i004p00851, 1982.

Miyazaki, K., Watanabe, S., Kawatani, Y., Sato, K., Tomikawa, Y., and Takahashi, M.: Transport and Mixing in the Extratropical Tropopause Region in a High-Vertical-Resolution GCM. Part II: Relative Importance of Large-Scale and Small-Scale Dynamics, Journal of the Atmospheric Sciences, 67, 1315–1336, https://doi.org/10.1175/2009JAS3334.1, http://journals.ametsoc.org/doi/abs/10.1175/2009JAS3334.1, 2010.

Morgenstern, O. and Carver, G. D.: Quantification of filaments penetrating the subtropical barrier, Journal of Geophysical Research Atmospheres, 104, 31 275–31 286, https://doi.org/10.1029/1999JD900792, 1999.

Müller, S., Hoor, P., Berkes, F., Bozem, H., Klingebiel, M., Reutter, P., Smit, H. G. J., Wendisch, M., Spichtinger, P., and Borrmann, S.: In situ detection of stratosphere-troposphere exchange of cirrus particles in the midlatitudes, Geophysical Research Letters, 42, 949–955, https://doi.org/10.1002/2014GL062556, 2015.

O'Sullivan, D. and Dunkerton, T. J.: Generation of Inertia–Gravity Waves in a Simulated Life Cycle of Baroclinic Instability, Journal of the Atmospheric Sciences, 52, 3695–3716, https://doi.org/10.1175/1520-0469(1995)052<3695:GOIWIA>2.0.CO;2, 1995.

Pan, L. L., Randel, W. J., Gary, B. L., Mahoney, M. J., and Hintsa, E. J.: Definitions and sharpness of the extratropical tropopause: A trace gas perspective, Journal of Geophysical Research, 109, D23 103, https://doi.org/10.1029/2004JD004982, 2004.

Pan, L. L., Wei, J. C., Kinnison, D. E., Garcia, R. R., Wuebbles, D. J., and Brasseur, G. P.: A set of diagnostics for evaluating chemistry-climate models in the extratropical tropopause region, Journal of Geophysical Research, 112, 1–12, https://doi.org/10.1029/2006JD007792, 2007.

Pepler, S. J., Vaughan, G., and Hooper, D. A.: Detection of turbulence around jet streams using a VHF radar, Quarterly Journal of the Royal Meteorological Society, 124, 447–462, https://doi.org/10.1002/qj.49712454605, 1998.

Poulida, O., Dickerson, R. R., and Heymsfield, A.: Stratosphere-troposphere exchange in a midlatitude mesoscale convective complex 1. Observations, Journal of Geophysical Research, 101, 6823–6836, https://doi.org/10.1029/95JD03523, 1996.

Reutter, P., Škerlak, B., Sprenger, M., and Wernli, H.: Stratosphere–troposphere exchange (STE) in the vicinity of North Atlantic cyclones, Atmospheric Chemistry and Physics, 15, 10 939–10 953, https://doi.org/10.5194/acp-15-10939-2015, 2015.

Riese, M., Ploeger, F., Rap, A., Vogel, B., Konopka, P., Dameris, M., and Forster, P.: Impact of uncertainties in atmospheric mixing on simulated UTLS composition and related radiative effects, Journal of Geophysical Research, 117, D16 305, https://doi.org/10.1029/2012JD017751, 2012.

Riese, M., Oelhaf, H., Preusse, P., Blank, J., Ern, M., Friedl-Vallon, F., Fischer, H., Guggenmoser, T., Höpfner, M., Hoor, P., Kaufmann, M., Orphal, J., Plöger, F., Spang, R., Suminska-Ebersoldt, O., Ungermann, J., Vogel, B., and Woiwode, W.: Gimballed Limb Observer for Radiance Imaging of the Atmosphere (GLORIA) scientific objectives, Atmospheric Measurement Techniques, 7, 1915–1928, https://doi.org/10.5194/amt-7-1915-2014, 2014.

Shapiro, M. A.: Turbulent Mixing within Tropopause Folds as a Mechanism for the Exchange of Chemical Constituents between the Stratosphere and Troposphere, Journal of the Atmospheric Sciences, 37, 994–1004, https://doi.org/10.1175/1520-0469(1980)037<0994:TMWTFA>2.0.CO;2, 1980.

Škerlak, B., Sprenger, M., and Wernli, H.: A global climatology of stratosphere–troposphere exchange using the ERA-Interim data set from 1979 to 2011, Atmospheric Chemistry and Physics, 14, 913–937, https://doi.org/10.5194/acp-14-913-2014, 2014.

Škerlak, B., Sprenger, M., Pfahl, S., Tyrlis, E., and Wernli, H.: Tropopause Folds in ERA-Interim: Global Climatology and Relation to Extreme Weather Events, Journal of Geophysical Research: Atmospheres, 120, n/a–n/a, https://doi.org/10.1002/2014JD022787, 2015.

Spreitzer, E., Attinger, R., Boettcher, M., Forbes, R., Wernli, H., and Joos, H.: Modification of Potential Vorticity near the Tropopause by Nonconservative Processes in the ECMWF Model, Journal of the Atmospheric Sciences, 76, 1709–1726, https://doi.org/10.1175/JAS-D-18-0295.1, 2019.

Sprenger, M. and Wernli, H.: The LAGRANTO Lagrangian analysis tool – version 2.0, Geoscientific Model Development, 8, 2569–2586, https://doi.org/10.5194/gmd-8-2569-2015, 2015.

Sprenger, M., Maspoli, M. C., and Wernli, H.: Tropopause folds and cross-tropopause exchange: A global investigation based upon ECMWF analyses for the time period March 2000 to February 2001, Journal of Geophysical Research, 108, 8518, https://doi.org/10.1029/2002JD002587, 2003.

Sprenger, M., Wernli, H., and Bourqui, M.: Stratosphere–Troposphere Exchange and Its Relation to Potential Vorticity Streamers and Cutoffs near the Extratropical Tropopause, Journal of the Atmospheric Sciences, 64, 1587–1602, https://doi.org/10.1175/JAS3911.1, 2007.

Stenchikov, G., Dickerson, R., Pickering, K., Ellis Jr., W., Doddridge, B., Kondragunta, S., and Poulida, O.: Stratosphere-troposphere exchange in a midlatitude mesoscale convective complex 2. Numerical simulations, Journal of Geophysical Research, 101, 6837–6851, https://doi.org/10.1029/95JD02468, 1996.

Steppeler, J., Doms, G., Schättler, U., Bitzer, H. W., Gassmann, A., Damrath, U., and Gregoric, G.: Meso-gamma scale forecasts using the nonhydrostatic model LM, Meteorology and Atmospheric Physics, 82, 75–96, https://doi.org/10.1007/s00703-001-0592-9, 2003.

Stohl, A., Bonasoni, P., Cristofanelli, P., Collins, W., Feichter, J., Frank, A., Forster, C., Gerasopoulos, E., Gäggeler, H., James, P., Kentarchos, T., Kromp-Kolb, H., Krüger, B., Land, C., Meloen, J., Papayannis, A., Priller, A., Seibert, P., Sprenger, M., Roelofs, G. J., Scheel, H. E., Schnabel, C., Siegmund, P., Tobler, L., Trickl, T., Wernli, H., Wirth, V., Zanis, P., and Zerefos, C.: Stratosphere-troposphere exchange: A review, and what we have learned from STACCATO, Journal of Geophysical Research: Atmospheres, 108, https://doi.org/10.1029/2002JD002490, 2003.

Tang, Q., Prather, M. J., and Hsu, J.: Stratosphere-troposphere exchange ozone flux related to deep convection, Geophysical Research Letters, 38, 1–5, https://doi.org/10.1029/2010GL046039, 2011.

Thorncroft, C. D., Hoskins, B. J., and McIntyre, M. E.: Two paradigms of baroclinic-wave life-cycle behaviour, Quarterly Journal of the Royal Meteorological Society, 119, 17–55, https://doi.org/10.1002/qj.49711950903, 1993.

Tiedtke, M.: A Comprehensive Mass Flux Scheme for Cumulus Parameterization in Large-Scale Models, Monthly Weather Review, 117, 1779–1800, https://doi.org/10.1175/1520-0493(1989)117<1779:ACMFSF>2.0.CO;2, 1989.

Tung, K. K. and Orlando, W. W.: The k^{-3} and $k^{-5/3}$ Energy Spectrum of Atmospheric Turbulence: Quasigeostrophic Two-Level Model Simulation, Journal of the Atmospheric Sciences, 60, 824–835, https://doi.org/10.1175/1520-0469(2003)060<0824:TKAKES>2.0.CO;2, 2003.

Ungermann, J., Blank, J., Dick, M., Ebersoldt, A., Friedl-Vallon, F., Giez, A., Guggenmoser, T., Höpfner, M., Jurkat, T., Kaufmann, M., Kaufmann, S., Kleinert, A., Krämer, M., Latzko, T., Oelhaf, H., Olchewski, F., Preusse, P., Rolf, C., Schillings, J., Suminska-Ebersoldt, O., Tan, V., Thomas, N., Voigt, C., Zahn, A., Zöger, M., and Riese, M.: Level 2 processing for the imaging Fourier transform spectrometer GLORIA: Derivation and validation of temperature and trace gas volume mixing ratios from calibrated dynamics mode spectra, Atmospheric Measurement Techniques, 8, 2473–2489, https://doi.org/10.5194/amt-8-2473-2015, 2015.

Vallis, G. K.: Atmospheric and Oceanic Fluid Dynamics, p. 964, https://doi.org/10.1017/9781107588417, 2017.

Wernli, H. and Bourqui, M.: A Lagrangian "1-year climatology" of (deep) cross-tropopause exchange in the extratropical Northern Hemisphere, Journal of Geophysical Research, 107, 4021, https://doi.org/10.1029/2001JD000812, 2002.

Wernli, H. and Davies, H. C.: A lagrangian-based analysis of extratropical cyclones. I: The method and some applications, Quarterly Journal of the Royal Meteorological Society, 123, 467–489, https://doi.org/10.1002/qj.49712353811, 1997.

Whiteway, J. A., Pavelin, E. G., Busen, R., Hacker, J., and Vosper, S.: Airborne measurements of gravity wave breaking at the tropopause, Geophysical Research Letters, 30, n/a–n/a, https://doi.org/10.1029/2003GL018207, 2003.

Whiteway, J. A., Klaassen, G. P., Bradshaw, N. G., and Hacker, J.: Transition to turbulence in shear above the tropopause, Geophysical Research Letters, 31, 2–5, https://doi.org/10.1029/2003GL018509, 2004.

Wirth, V.: Diabatic heating in an axisymmetric cut-off cyclone and related stratosphere-troposphere exchange, Quarterly Journal of the Royal Meteorological Society, 121, 127–147, https://doi.org/10.1002/qj.49712152107, 1995.

WMO: Meteorology - A three dimensional science, WMO Bulletin, pp. 134–138, 1957.

Zhang, F., Wei, J., Zhang, M., Bowman, K. P., Pan, L. L., Atlas, E., and Wofsy, S. C.: Aircraft measurements of gravity waves in the upper troposphere and lower stratosphere during the START08 field experiment, Atmospheric Chemistry and Physics, 15, 7667–7684, https://doi.org/10.5194/acp-15-7667-2015, 2015a.

Zhang, Y., Zhang, S., Huang, C., Huang, K., Gong, Y., and Gan, Q.: The Interaction between the Tropopause Inversion Layer and the Inertial Gravity Wave activities revealed by radiosonde observations at a midlatitude station, Journal of Geophysical Research: Atmospheres, pp. n/a–n/a, https://doi.org/10.1002/2015JD023115, 2015b.

Zierl, B. and Wirth, V.: The influence of radiation on tropopause behavior and stratosphere-troposphere exchange in an upper tropospheric anticyclone, Journal of Geophysical Research, 102, 23 883, https://doi.org/10.1029/97JD01667, 1997.